Journal of Environmental Chemical Engineering 14 (2026) 121773

Contents lists available at ScienceDirect

Journal of Environmental Chemical Engineering

journal homepage: www.elsevier.com/locate/jece

Selective fixed-bed fractionation of stilbene subfamilies from grape cane waste using a pyridine-amide adsorbent

Amir Bzainia [a,b], Erik Keller [c], André Heeres [c], Mário Rui P.F.N. Costa [b], Rolando C.S. Dias [a,*]

[a] Centro de Investigação de Montanha (CIMO), Instituto Politécnico de Bragança, Campus de Santa Apolónia, Bragança 5300-253, Portugal
[b] Faculdade de Engenharia da Universidade do Porto, Rua Roberto Frias s/n, Porto 4200-465, Portugal
[c] Hanze University of Applied Sciences, Zernikeplein 7, Groningen 9747 AS, the Netherlands

ARTICLE INFO

Keywords:
Grape canes
Stilbenes
Poly(BAAPy)
Fixed-bed adsorption
Biomass valorisation
Phytochemical recovery
Subfamily-selective separation

ABSTRACT

The selective separation of structurally analogous polyphenols from complex plant matrices remains a long-standing challenge in bioseparation engineering. This study introduces a custom-designed adsorbent, poly(2,6-bis(acrylamido)pyridine) (poly(BAAPy)), tailored for subfamily-level resolution of stilbenes obtained from crude grape cane extracts. Leveraging dual amide and pyridine functionalities, poly(BAAPy) achieves selective retention of oligomeric stilbenes (e.g., trans-ε-viniferin, miyabenol C) via multivalent hydrogen bonding and π-π stacking interactions. Comparative breakthrough experiments against commercial poly(4-vinylpyridine) (poly(4VP)) demonstrate superior oligomer retention across both ethanol-water and acetonitrile systems. In dynamic closed-loop adsorption mode, poly(BAAPy) enabled polarity-driven elution and achieved up to a 3.4-fold enrichment of stilbene oligomers, with their recovery in fractions containing ≥ 90 % oligomeric content in a single desorption cycle. Uptake profiles and adsorption selectivity coefficients confirmed poly(BAAPy)'s preference for oligomers under both ethanol-water and acetonitrile conditions. The total stilbene recovery was 75 %. Breakthrough data were fitted using both empirical (Clark, Thomas) and mechanistic models, revealing distinct adsorption dynamics for poly(BAAPy) versus a commercial poly(4VP) resin. This work demonstrates a sustainable valorisation route for grape cane waste, converting viticultural residues into a high-value source of bioactive compounds. The use of green solvents and fixed-bed adsorption aligns with circular economy principles and environmentally conscious separation processes.

1. Introduction

Selective downstream separation of structurally similar phenolic bioactive compounds remains a bottleneck in green extraction workflows and sustainable phytochemical valorisation. Among these, stilbene-based phenolic metabolites have attracted attention due to their potent antioxidant, anti-inflammatory [1], and anticancer properties [2], making them promising candidates for applications in nutraceuticals, pharmaceuticals, and food preservation. Stilbenes are particularly abundant in grapevine-derived biomass, including grape canes [3,4].

Among the polyphenols derived from grapes, stilbene oligomers such as trans-ε-viniferin and miyabenol C, have shown superior bioactivity compared to monomeric analogues like trans-resveratrol. These oligomers exhibit enhanced radical scavenging efficiency [5] and synergistic antioxidant activity in the presence of other stilbenes [6]. Furthermore, tetrameric structures, such as vaticanol C, have also demonstrated 4–7-fold greater cytotoxicity than trans-resveratrol in cancer models [7].

Despite their bioactivity, the efficient isolation of stilbenes, especially oligomeric forms, from crude natural extracts remains a considerable challenge. Ethanol-water extractions typically lead to co-extraction of various compounds such as sugars, tannins, and proteins, which often form non-specific complexes with stilbenes [8,9]. This co-extraction complicates separation efforts, and conventional chromatographic techniques frequently lack the selectivity needed to resolve stilbene subfamilies with subtle structural differences [10–13].

Traditionally, the isolation of stilbene oligomers has relied on methods such as high-speed counter-current chromatography (HSCCC) [14], medium-pressure liquid chromatography, and semipreparative high-performance liquid chromatography [15]. Other approaches, such as centrifugal partition chromatography (CPC), have also demonstrated subfamily-level resolution of stilbene oligomers using biphasic solvent

* Corresponding author.
E-mail address: rdias@ipb.pt (R.C.S. Dias).

https://doi.org/10.1016/j.jece.2026.121773
Received 19 October 2025; Received in revised form 1 February 2026; Accepted 11 February 2026
Available online 12 February 2026

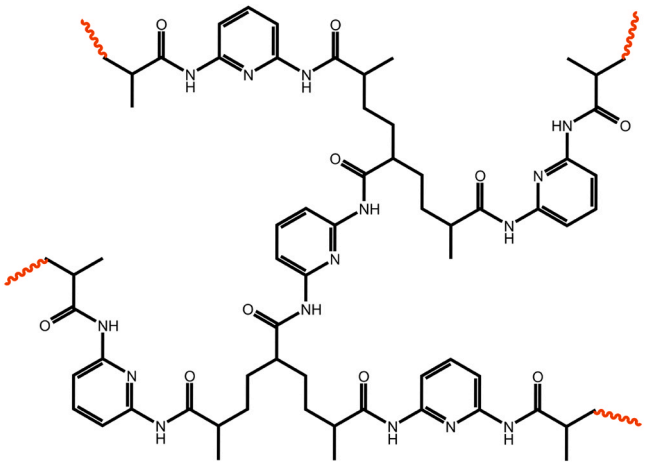

Fig. 1. Chemical structure of poly(2,6-bis(acrylamido)pyridine) (poly(BAAPy)).

systems and stepwise elution gradients [16,17]. These techniques are highly effective for fine resolution and purification, including the isolation of individual compounds, but they typically require careful solvent-system selection and optimisation and can become operationally demanding when processing complex crude natural extracts. In this context, subfamily-level fractionation/enrichment (e.g., separating monomeric from oligomeric stilbenes) can serve as a practical upstream step to simplify the matrix and concentrate targeted subclasses, either for direct use where enriched mixtures are acceptable, or as a feed stream better suited for subsequent high-resolution purification (e.g., HSCCC/CPC) when single-compound purity is required.

As a potential alternative to multi-step chromatographic separations, adsorption-based techniques offer advantages in operational simplicity, scalability, and solvent efficiency [18]. Functionalized polymer adsorbents are increasingly applied for selective capture and release of bioactive compounds, particularly in food and environmental engineering [19,20]. Importantly, porous polymer resins (e.g., polyamide-type and related sorbents) have long been used as practical workhorse materials for bulk uptake and pre-concentration of polyphenols from complex plant matrices, where performance is often driven by non-specific hydrophobic and π–π contributions and by hydrogen bonding to polar sites [21]. To improve selectivity, more tailored polymeric platforms—such as molecularly imprinted sorbents designed for enrichment and scale-up sorption workflows [22] and functionalized adsorbents reported for continuous purification of stilbenes from grape-derived biomass [23]—have been developed. Likewise, pyridyl-functionalized sorbents operating in hydroalcoholic media have been shown to enhance affinity-driven separation of bioactives from natural extracts [24]. Nevertheless, most current studies focus on equilibrium adsorption under simplified conditions, and their application to realistic multicomponent systems, such as natural grape cane extracts, remains limited.

To address these limitations, we investigated a novel polymer adsorbent, poly(2,6-bis(acrylamido)pyridine) (poly(BAAPy)) (see Fig. 1), for dynamic fixed-bed fractionation of stilbene subfamilies from grape cane extracts. The BAAPy monomer contains two amide groups and an electron-rich pyridine ring, facilitating multivalent hydrogen bonding, π-π stacking, and other non-covalent interactions (e.g., hydrophobic effects) with stilbenes. To our knowledge, no previous study has reported the use of poly(BAAPy) for dynamic fixed-bed separations, nor its application in recovering bioactive compounds from natural sources.

In this study, we evaluate the adsorption performance of poly (BAAPy) in comparison to a commercial poly(4-vinylpyridine)-based resin (Reillex® 402), whose monomeric unit, 4-vinylpyridine (4VP), is frequently used in polyphenol separations, particularly in molecularly imprinted and grafted polymer systems [25–27]. The structural similarity between BAAPy and 4VP enables a direct comparison of adsorption behaviours governed by functional group interactions.

Recognizing the chemical complexity and growing potential of grape cane extracts as a renewable feedstock, we assess the capacity of both polymers to selectively retain and fractionate stilbene subfamilies, including monomeric (e.g., trans-resveratrol) and oligomeric (e.g., trans-ε-viniferin) compounds, under dynamic fixed-bed conditions. Adsorption behaviour was characterized through breakthrough and desorption experiments in open-loop configurations using two solvent systems, enabling the assessment of subfamily-specific retention and elution profiles. To evaluate scalability, closed-loop dynamic adsorption was carried out using an ethanol–aqueous extract, followed by a stepwise solvent elution. This process allowed the fractionation of stilbenes into monomeric and oligomeric families using poly(BAAPy). The composition of each eluted fraction and corresponding enrichment factors were quantified to differentiate the performance of poly(BAAPy) from that of poly(4VP), highlighting its capability for subfamily-level separation.

This study advances current stilbene separation strategies by introducing a pyridine–amide bifunctional adsorbent (poly(BAAPy)) evaluated under dynamic fixed-bed operation, a configuration that is directly compatible with scalable downstream processing because it enables controlled empty-bed contact time, straightforward fraction collection, and efficient bed reconditioning via programmed solvent switching. Under these flow conditions, performance is governed by convective mass transfer, competitive adsorption in complex matrices, and polarity-driven desorption rather than equilibrium batch behaviour. Beyond demonstrating preferential retention of oligomeric stilbenes, we provide a process-relevant framework—open-loop breakthrough/desorption in two solvent systems and a closed-loop fractionation scheme—quantified using selectivity coefficients, enrichment factors, and overall recovery. In this way, poly(BAAPy) is positioned as a scalable fractionation and pre-concentration step for grape-cane-derived stilbenes, producing monomer- and oligomer-enriched fractions that can be used directly where mixture enrichment is sufficient, or integrated upstream of high-resolution methods when single-compound purity is required.

2. Experimental part

2.1. Reagents and solvents

2,2′-azobis(2-methylpropionitrile) (AIBN, ≥ 98 %, CAS: 78–67–1) was supplied by Sigma Aldrich (Germany). Dimethylformamide (DMF, ≥ 99 %, CAS: 68–12–2) was acquired from Acros Organics (Belgium). Standards for trans-resveratrol (t-resveratrol, ≥ 98 %, CAS: 501–36–0) and trans-epsilon-viniferin (t-ε-viniferin, ≥ 90 %, CAS: 62218–08–0) were purchased from Cayman (USA). Ethanol (≥ 99.8 %, CAS: 64–17–5), acetonitrile (ACN, ≥ 99.9 %, CAS: 75–05–8), acetone (≥ 99.8 %, CAS: 67–64–1), ethyl acetate (≥ 99.8 %, CAS: 141–78–6), methanol (≥ 99.8 %, CAS: 67–56–1) and acetic acid (≥ 99.7 %, CAS: 64–19–7) were sourced from Fisher Scientific (UK). Ultrapure water used in all experiments was obtained from an in-house purification system.

2.2. Synthesis and characterization of Poly(BAAPy)

Poly(BAAPy) was synthesized via free-radical polymerization of a bis-amide pyridine monomer, following our previously reported method [28]. The polymerization was carried out in an ACN/DMF (7:3) mixture at 60 °C for 24 h under argon, using 5 mol% AIBN as initiator. The polymer was washed with methanol and dried under vacuum. Full synthetic details, monomer preparation, and FTIR analysis are provided in Supporting Information S1.

Scanning electron microscopy (SEM) was used to examine the

Table 1
Grape cane varieties used in this study along with their origin denominations and geographic distribution across Portugal.

Grape Cane Variety	Tinta Amarela	Tinta Francisco	Tinta Roriz	Tinta Cão	Touriga Nacional	Touriga Franca	Bastardo	Sousão
Region of Origin	Alentejo, Douro, Dão	Douro	Douro, Dão, Alentejo	Douro, Dão	Douro, Dão, Bairrada, Beira Interior	Douro	Douro, Dão, Madeira	Douro, Vinho Verde (Minho)

surface morphology of poly(BAAPy). Analyses were performed at the International Iberian Nanotechnology Laboratory (INL), Braga (Portugal), using a Helios Nanolab 450S FIB/SEM. SEM micrographs were acquired using an accelerating voltage of 15 kV (ETD detector) at a working distance of 9.6 mm, using magnifications from 1000 × to 50000 × .

The specific surface area and pore volume of the produced poly (BAAPy) adsorbent particles were determined through N2 adsorption/desorption isotherms at 77 K using a Micrometrics TriStar II Plus 3.03 adsorption analyzer, Malvern Panalytical. The same measurements were performed for the Reillex® 402 adsorbent. These N2 adsorption/desorption measurements were performed at the department of Chemistry and Biochemistry of the Faculty of Sciences of the University of Porto (FCUP), Porto, Portugal.

2.3. Extraction of Stilbenes from Grape Canes

Eight grape cane varieties were harvested in March 2024 from the Polytechnic Institute of Bragança vineyard. Specifically, the set was chosen to cover multiple major Portuguese wine regions (Table 1) and include cultivars with different viticultural relevance (widely cultivated and regionally representative varieties), so that the stilbene screening reflects realistic feedstock variability expected in grape-cane waste streams. The grape canes were stored for two months at room temperature in a dry, dark environment, then cut into ~3 cm segments, and ground to hay-like consistency using a micro-plant grinder (VARANDAS Z.M.A, MAZI). Extraction was carried out using ethanol-water (8:2, v/v) at a 1:10 (g/mL) biomass-to-solvent ratio, with ultrasound assistance (10 min) followed by shaking (150 rpm, 2 h). Three consecutive extractions using the same batch of variety were performed to assess the content of stilbenes per dry weight of grape canes. The same procedure was also applied using ACN.

2.4. HPLC Analysis

Extracts and collected fractions were analysed by HPLC–DAD. trans-Resveratrol and trans-ε-viniferin were identified by retention-time and UV–Vis spectral matching against authentic reference standards. For t-piceatannol and miyabenol C, assignments were made using DAD spectral profiles and retention behaviour consistent with reported stilbene signatures in Vitis vinifera matrices; the corresponding UV spectra recorded in this study are provided in Supporting Information (Figure S2). For quantification, external calibration curves were established for trans-resveratrol and trans-ε-viniferin (Supporting Information, Figures S3–S4), with linear range, regression equations, R^2, and calculated LOD/LOQ reported in Table S1. Peak areas were integrated using compound-specific DAD channels selected from the standards' absorbance maxima under the applied conditions (trans-resveratrol: 306 nm; trans-ε-viniferin: 324 nm). When commercial standards were not available, t-piceatannol was quantified as trans-resveratrol equivalents and miyabenol C as trans-ε-viniferin equivalents, assuming comparable DAD response for closely related stilbenes; values are therefore reported as mg L^{-1} equivalents and used consistently for enrichment and recovery calculations.

Chromatographic analysis was conducted using an Ascentis C18 column (Supelco®) with a particle size of 5 µm and dimensions of 25 cm × 4.6 mm. The mobile phase consisted of a solvent gradient ranging from 90 % water (adjusted to a pH of 3 with acetic acid) to 100 % ACN

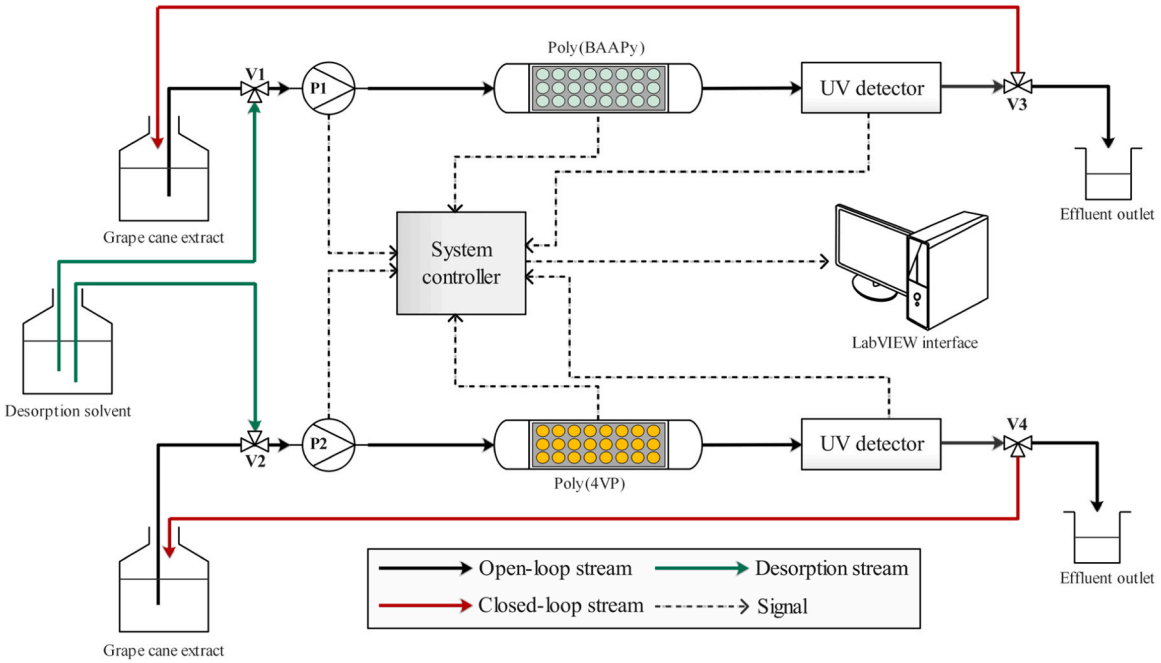

Fig. 2. Schematic diagram of the dual-line fixed-bed adsorption system used for stilbene fractionation. Columns packed with either poly(BAAPy) and commercial poly(4VP) were connected to independent pumps (P1, P2), UV detectors, and flow-control valves (V1-V4). System control and data acquisition were handled via LabVIEW® software.

over 25 min. The column temperature was maintained at 45°C, and the flow rate at 1 mL/min.

2.5. Fixed-bed adsorption experiments

2.5.1. Setup and operation

Poly(BAAPy) was packed into stainless-steel column (50 mm length × 20 mm I.D., 2.32 g total weight). Poly(4VP) resin (Reillex® 402, 22 g) was packed in a similar way (250 mm length × 20 mm I.D). The poly (4VP) resin was selected for comparison due to its established use in phenolic separations and its 98 % 4-vinylpyridine composition. Both columns were used in parallel in a dual-line fixed-bed system developed with the Portuguese company PARALAB. Each line included a pump, valve, and UV detector, all controlled by LabVIEW® software. Column temperature and data acquisition were fully automated. The schematic depiction of the experimental setup is shown in Fig. 2. To ensure fair comparison, equivalent empty bed contact times (EBCT) of 20.9 min were used. This corresponded to flow rates of 0.75 mL/min for poly (BAAPy) and 3.75 mL/min for poly(4VP), adjusted for column geometry (Supporting Information S5). This approach follows standard fixed-bed design practices, ensuring equivalent residence times across columns with differing geometries [29,30].

2.5.2. Adsorption selectivity assessment

A selectivity coefficient was calculated to quantify each adsorbent's affinity toward different stilbene subfamilies, using a model adapted from gas-phase separation theory [31]. Stilbenes were grouped into:

- Monomers: t-piceatannol and t-resveratrol
- Oligomers: t-ε-viniferin (dimer) and miyabenol C (trimer).

The selectivity of oligomeric over monomeric stilbenes was defined as:

$$S_{Oligomers/Monomers} = \frac{\left(Q_{viniferin} + Q_{miyabenol\ C}\right)/\left(Q_{resveratrol} + Q_{piceatannol}\right)}{\left(C_{viniferin} + C_{miyabenol\ C}\right)/\left(C_{resveratrol} + C_{piceatannol}\right)}$$

Where Q_i and C_i represent the adsorbed amount (mg/g) and the feed concentration (mg/L), respectively, of compound *i*. A value of $S_{oligomers/Monomers}$ greater than 1 indicates preferential adsorption of oligomeric stilbenes, while values < 1 indicate higher retention of monomeric ones.

In acetonitrile grape cane extracts, t-piceatannol was not detected. Therefore, both its feed concentration and adsorbed quantity were set to zero in the selectivity calculation for that condition.

2.5.3. Open-Loop adsorption using grape cane extracts

Breakthrough experiments were conducted over 20 bed volumes using grape cane extracts prepared in both acetonitrile (ACN) and ethanol-water (1:1, v/v) as feed solvents. For ethanol–water experiments, the crude extract initially obtained in ethanol–water (8:2, v/v) was diluted with ultrapure water to ethanol–water (1:1, v/v) prior to column loading. Adsorption was performed at 15 °C, and effluent samples were analysed using HPLC-DAD. The desorption sequence was conducted at 45 °C, beginning with 100 % water and followed by ethanol-water mixtures with increasing ethanol concentrations in 20 % (v/v) increments, up to 100 % ethanol. Final desorption steps were carried out using acetone and ethyl acetate. Each elution step covered 2 bed volumes, and all collected fractions were analysed by HPLC-DAD. This desorption solvent sequence also serves as the bed-regeneration step prior to subsequent adsorption runs by removing retained stilbenes and re-equilibrating the column to the initial solvent conditions.

2.5.3.1. Quantification of Stilbene Uptake. The uptake of each stilbene compound was quantified as the normalized amount adsorbed relative to the initial feed concentration (Q/C_0). The collected effluent samples analysed by HPLC-DAD allowed to determine the concentrations of t-piceatannol, t-resveratrol, t-ε-viniferin, and miyabenol C. The uptake was calculated using the following equation:

$$\frac{Q}{C_0} = \frac{(C_0 - C_{out})\ BV\ V_b}{m\ C_0}$$

Where C_0 and C_{out} feed and effluent concentrations (mg/L); BV is the number of bed volumes passed at each sampling point; V_b is the bed volume (mL); and m is the mass of adsorbent (g).

2.5.4. Closed-Loop Adsorption for Stilbenes Fractionation

A closed-loop dynamic adsorption system was implemented to simulate recirculating fixed-bed separation processes. In this setup, the column effluent was continuously recirculated into the feed reservoir. Adsorption was performed using ethanol-water (1:1, v/v) system at 15 °C, under the same empty-bed contact time (EBCT) described previously. Following adsorption, a discrete gradient-based desorption protocol was applied at 45°C to fractionate the retained stilbenes. Each desorption step was performed over 4 bed volumes. The elution sequence began with 100 % water and progressed through ethanol-water mixtures with increasing ethanol content in 10 % increments up to 100 % ethanol. This stepwise gradient was selected empirically, guided by a polarity/eluotropic-strength rationale: water-rich steps promote elution of weakly retained constituents, whereas progressively higher ethanol content increases desorption strength for more strongly retained stilbenes. A short final strong-solvent sequence (acetone, ethyl acetate, and MeOH–acetic acid, 9:1 v/v) was applied to ensure complete elution of the most retained compounds and to recondition the bed prior to reuse.

2.5.4.1. Quantitative Analysis of Stilbene Subfamily Enrichment Across Elution Fractions. To evaluate selective elution behaviour, each desorption fraction was analysed by HPLC-DAD to determine the relative distribution of stilbene subfamilies. Specifically, the proportion of monomeric stilbenes (t-piceatannol and t-resveratrol) and oligomeric stilbenes (t-ε-viniferin and miyabenol C) were calculated for each eluted fraction using the following expressions:

$$R_{Oligomers/Monomers} = \frac{C_{viniferin} + C_{miyabenol\ C}}{C_{resveratrol} + C_{piceatannol} + C_{viniferin} + C_{miyabenol\ C}}$$

$$R_{Monomers/Oligomers} = \frac{C_{resveratrol} + C_{piceatannol}}{C_{resveratrol} + C_{piceatannol} + C_{viniferin} + C_{miyabenol\ C}}$$

Where C_i denotes the concentration (mg/L) of stilbene *i* in each respective eluted fraction.

To assess enrichment or depletion relative to the original feed, enrichment factors were calculated as:

$$E_{Oligomers/Monomers} = \frac{R^{Fraction}_{Oligomers/Monomers}}{R^{Extract}_{Oligomers/Monomers}} \text{ and} E_{Monomers/Oligomers} = \frac{R^{Fraction}_{Monomers/Oligomers}}{R^{Extract}_{Monomers/Oligomers}}$$

These factors quantify the degree to which a given stilbene subclass was enriched or depleted in each elution fraction relative to the feed extract. Values greater than 1 indicate enrichment, whereas values less than 1 indicate depletion.

In addition to enrichment factors, total stilbene recovery (%) was calculated using:

$$Recovery\ (\%) = \left(\frac{\sum C_i\ V_i}{(C_{feed,\ \ initial} - C_{feed,\ \ final}) \times V_{feed}}\right) \times 100$$

where C_i is the total stilbenes concentration in the eluted *i*-th fraction, and V_i is the corresponding volume of that elution step. $C_{feed,initial}$ and $C_{feed,final}$ represent the stilbene concentrations in the feed reservoir before and after adsorption, respectively. V_{feed} denotes the total feed volume used in the closed-loop system.

Table 2
Non-linear kinetic models used to describe breakthrough behaviour in fixed-bed column systems. Models include Thomas, Yoon-Nelson, Bohart-Adams, Clark, and Modified Dose-Response (MDR). Equations are expressed as a function of bed volume (BV), with associated variable definitions provided.

Kinetic Model	Non-Linear Form	Parameter Definitions
Thomas	$\frac{C}{C_0} = \frac{1}{1+\exp\left(\frac{k_{Th}\,q_F m}{F} - \frac{k_{Th}C_0V_b}{F}BV\right)}$	k_{Th}: Thomas rate constant (mL/min·mg), q_F: adsorption capacity (mg/g), m: adsorbent mass (g)
Yoon-Nelson	$\frac{C}{C_0} = \frac{1}{1+\exp\left[k_{YN}\left(\tau - \frac{V_bBV}{F}\right)\right]}$	k_{YN}: rate constant (1/min), τ: time at 50 % breakthrough (min)
Bohart-Adams	$\frac{C}{C_0} = \frac{1}{1+\exp\left(\frac{k_{BA}N_0Z}{u} - \frac{k_{BA}C_0V_b}{F}BV\right)}$	k_{BA}: kinetic constant (L/mg min), N_0: saturation concentration (mg/L), Z: bed height (cm), u: linear velocity (cm/min)
Clark	$\frac{C}{C_0} = \left(\frac{1}{1+A\exp\left(-\frac{K_C V_b}{F}BV\right)}\right)^{\frac{1}{n-1}}$	A: empirical constant, K_C: Clark constant (1/min), n: Freundlich constant
Modified Dose-Response	$\frac{C}{C_0} = \frac{1}{1+\left(\frac{C_0\,V_bBV}{q_F m}\right)^{a'}}$	a′: empirical model constant, q_F: adsorption capacity (mg/g), m: adsorbent mass (g)

2.6. Kinetic Modelling of Stilbene Retention from Grape Cane Extracts

To describe the adsorption dynamics of stilbenes on poly(BAAPy) and poly(4VP), experimental breakthrough curves were fitted using five established fixed-bed kinetic models: Thomas, Yoon-Nelson, Bohart-Adams, Clark, and the Modified Dose-Response [32].

Nonlinear regression was performed in MATLAB using the built-in *lsqcurvefit* function, which applies a least-squares optimization algorithm to minimize the difference between experimental and predicted concentrations (C/C_0). All models were formulated as a function of bed volumes (*BV*), using the transformation

$$t = \frac{BV\,V_b}{F}$$

where F is the volumetric flowrate (mL/min) and V_b is the bed volume (mL). All modelling was based on mass concentrations (mg/L), consistent with industrial practice, where purification yield and product recovery are typically reported in weight-based terms. The mathematical expressions of the models are summarized in Table 2. To complement the empirical models, a mechanistic simulation based on the macroscopic mass balance for fixed-bed adsorption columns was also developed. This model incorporates axial dispersion, intraparticle mass transfer approximated by the Linear Driving Force (LDF) model, and non-linear single-site Langmuir adsorption equilibrium. Full mathematical derivations, boundary conditions, and numerical implementation are provided in the Supporting Information S6.

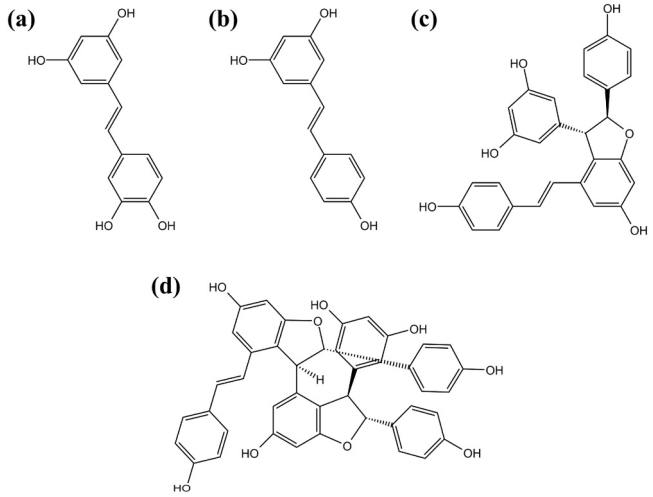

Fig. 4. Chemical structures of stilbenes identified in grape cane extracts. Monomers: (a) t-piceatannol, (b) t-resveratrol; Oligomers: (c) t-ε-viniferin, and (d) miyabenol C.

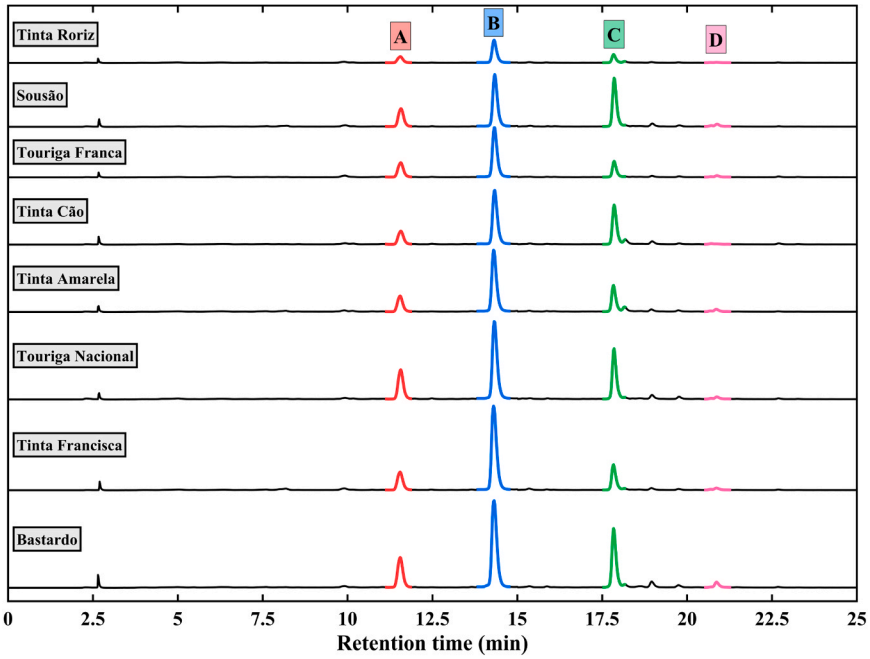

Fig. 3. HPLC-DAD chromatograms (λ = 320 nm) of ethanol-water (8:2, v/v) grape cane extracts from eight Portuguese cultivars. Stilbene peaks identified include: (A) t-piceatannol; (B) t-resveratrol; (C) t-ε-viniferin; and (D) miyabenol C.

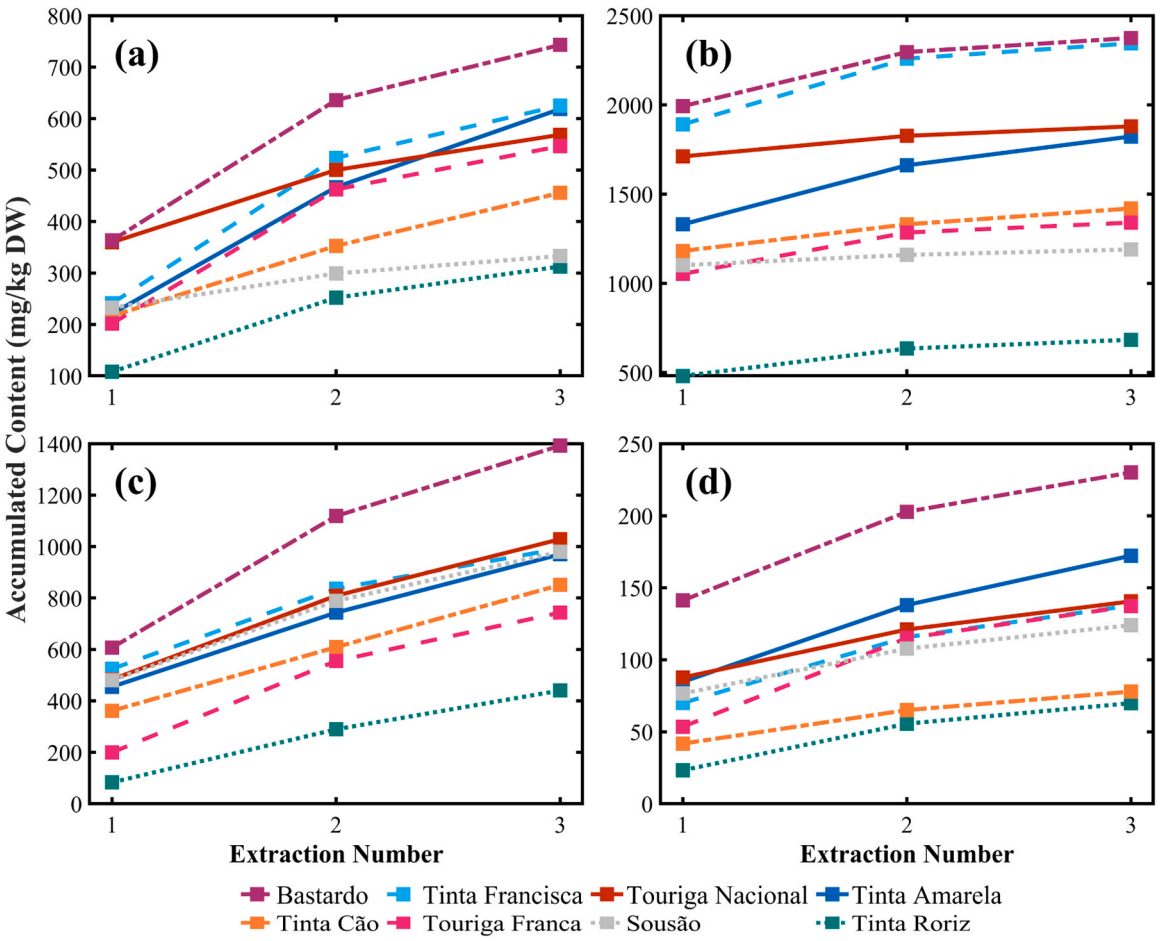

Fig. 5. Accumulated content (mg/kg DW) of extracted stilbenes from grape canes after three successive extractions using ethanol-water (8:2, v/v). Compounds quantified include: (a) t-piceatannol; (b) t-resveratrol; (c) t-ε-viniferin; and (d) miyabenol C.

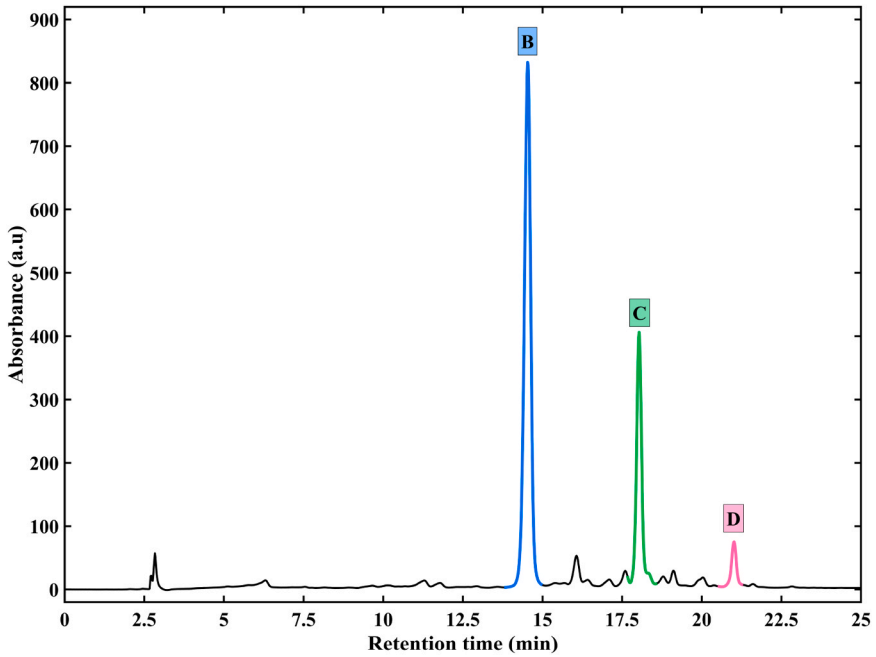

Fig. 6. HPLC-DAD chromatogram (λ = 320 nm) of grape cane extract obtained using acetonitrile (ACN) as the extraction solvent. Peaks correspond to: (B) t-resveratrol, (C) t-ε-viniferin, and (D) miyabenol C. t-Piceatannol was not detected under ACN extraction conditions.

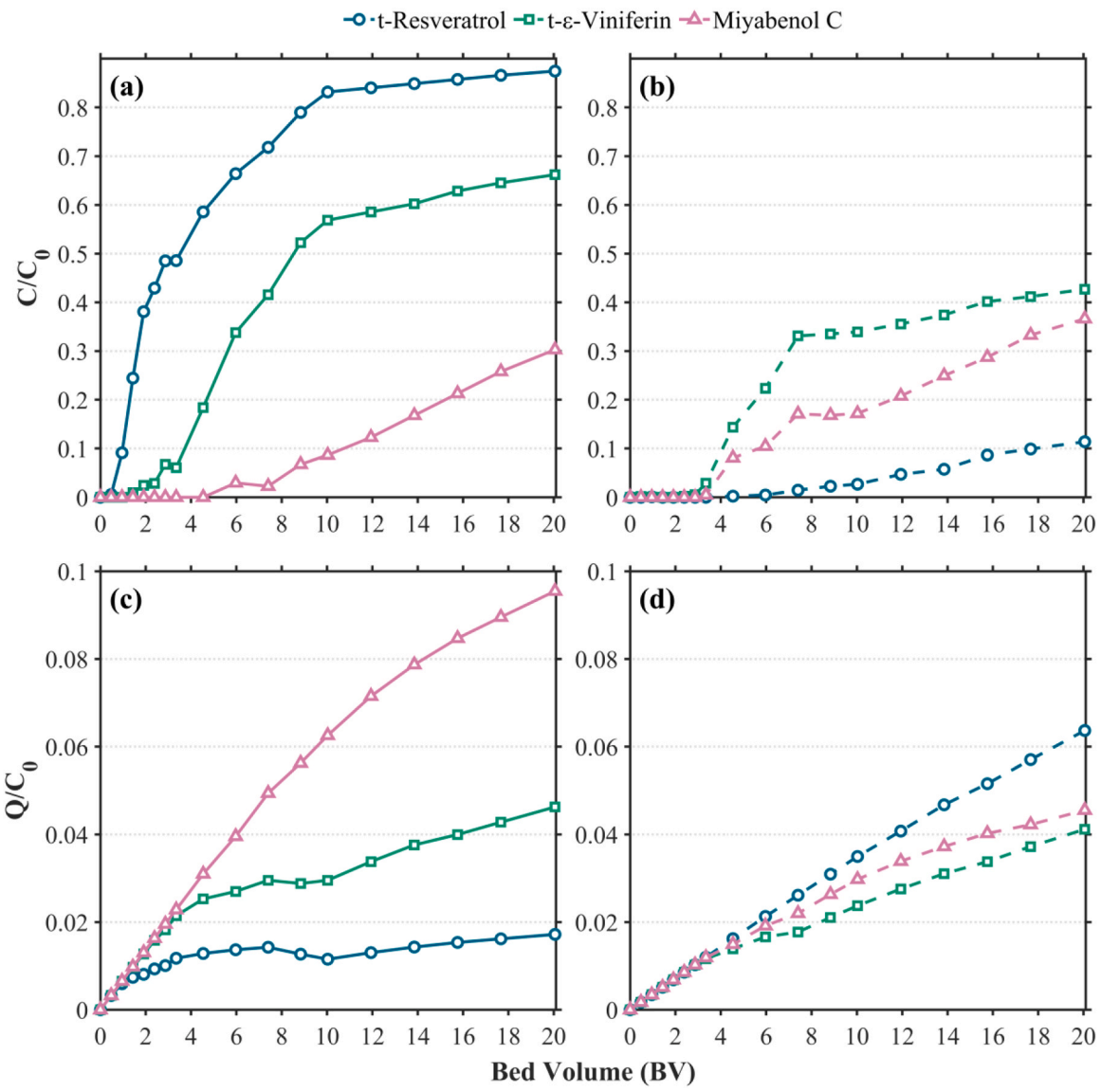

Fig. 7. Dynamic adsorption behaviour of stilbenes, t-resveratrol, t-ε-viniferin, and miyabenol C, on poly(BAAPy) and commercial poly(4VP) resin under acetonitrile (ACN) feed conditions. Panels (a) and (b) show breakthrough curves (C/C_0), while panels (c) and (d) display cumulative uptake (Q/C_0). Data correspond to poly (BAAPy) in (a) and (c), and poly(4VP) in (b) and (d).

3. Results and discussion

3.1. Stilbene content in grape cane cultivars

The HPLC-DAD chromatograms of ethanol-water extracts from eight Portuguese grape cane varieties (Fig. 3) revealed four predominant stilbenes across all cultivars: t-piceatannol, t-resveratrol, t-ε-viniferin, and miyabenol C, corresponding to peaks A-D. The chemical structures of these compounds are shown in Fig. 4. Based on structural classification, t-piceatannol and t-resveratrol were identified as monomeric stilbenes, whereas t-ε-viniferin (a dimer of t-resveratrol) and miyabenol C (a trimer) were categorized as stilbene oligomers.

The identification of t-resveratrol and t-ε-viniferin was confirmed using analytical standards. For t-piceatannol and miyabenol C, compound identity was verified via UV absorption (Supporting Information S2), consistent with literature values. The UV spectrum of t-piceatannol matched that reported by Pezet et al. [33], while miyabenol C matched the profile reported by Papastamoulis et al. [34] for *Vitis vinifera*-derived extracts. This identification procedure followed the same validated methodology previously applied by our group for phenolic compound identification [35,36].

Fig. 5 illustrates the accumulated content of each stilbene after three successive ethanol-water (8:2, v/v) extraction cycles. The first extraction yielded the highest proportion of stilbenes, indicating efficient release of readily accessible compounds. Although yields continued to increase slightly, the third cycle recovered less than 15 % additional stilbenes on average, reflecting diminishing returns. Since complete biomass exhaustion was not the objective, the three-cycle protocol was selected to balance recovery and resource use, while ensuring a representative extract for downstream adsorption comparisons. The total stilbene content per cultivar is summarized in the Supporting Information S4 (Figure S6). Among the tested cultivars, 'Bastardo' and 'Tinta Francisca' exhibited the highest cumulative stilbene content, with t-resveratrol and t-ε-viniferin concentrations exceeding 2200 mg/kg DW and 1400 mg/kg DW, respectively. In contrast, 'Tinta Roriz' exhibited the lowest yields for all stilbenes, suggesting varietal differences in phenolic biosynthesis. These elevated stilbene levels reinforce the valorisation potential of grape cane biomass as a sustainable source of bioactive compounds.

To further evaluate the intrinsic adsorption affinities of the

Table 3
Stilbene adsorption selectivity coefficients for oligomeric vs. monomeric stilbenes for poly(BAAPy) and poly(4VP) adsorbents in ACN system. Values > 1 indicate preference toward a specific family.

Solvent System	Adsorbent	$S_{Oligomers/Monomers}$
Acetonitrile	Poly(BAAPy)	2.00
	Poly(4VP) commercial resin	0.84

adsorbents, and to decouple solvent effects from polymer-stilbene interactions, acetonitrile (ACN) was employed as an alternative extraction solvent. The accumulated total stilbene content obtained after three successive ACN extraction cycles (representative variety) is provided in the Supporting Information S4 (Figure S7). Due to its lower polarity and weaker hydrogen-bonding capacity compared to aqueous ethanol, ACN minimizes nonspecific interactions with the adsorbent. The resulting chromatogram (Fig. 6) revealed three main stilbene peaks

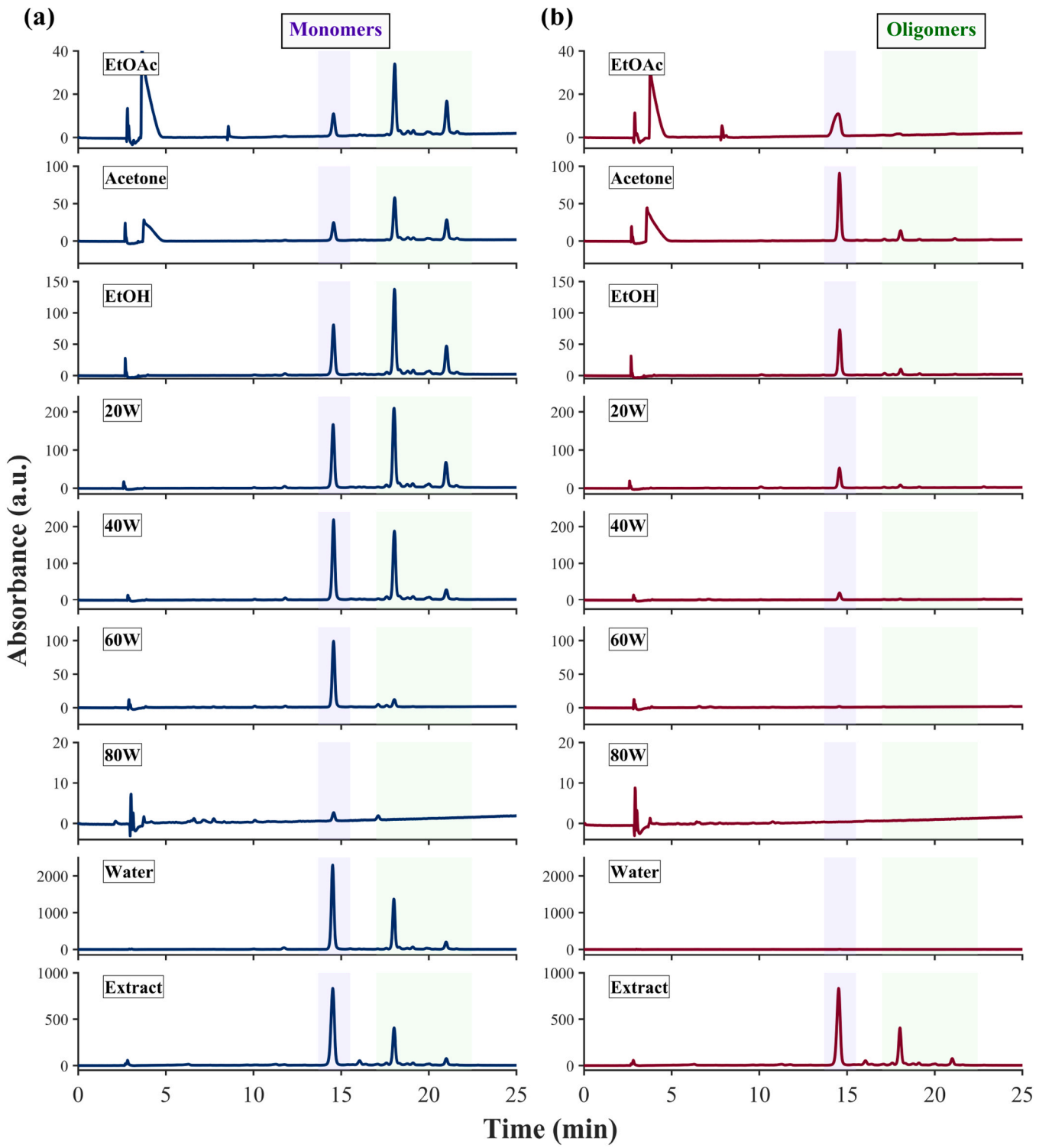

Fig. 8. Desorption chromatograms (λ = 320 nm) of ACN-based grape cane extract eluted from (a) poly(BAAPy) and (b) poly(4VP) columns. Desorption was performed from water to ethyl acetate (EtOAc) in stepwise polarity gradients. Shaded regions highlight the elution of monomeric versus oligomeric stilbenes.

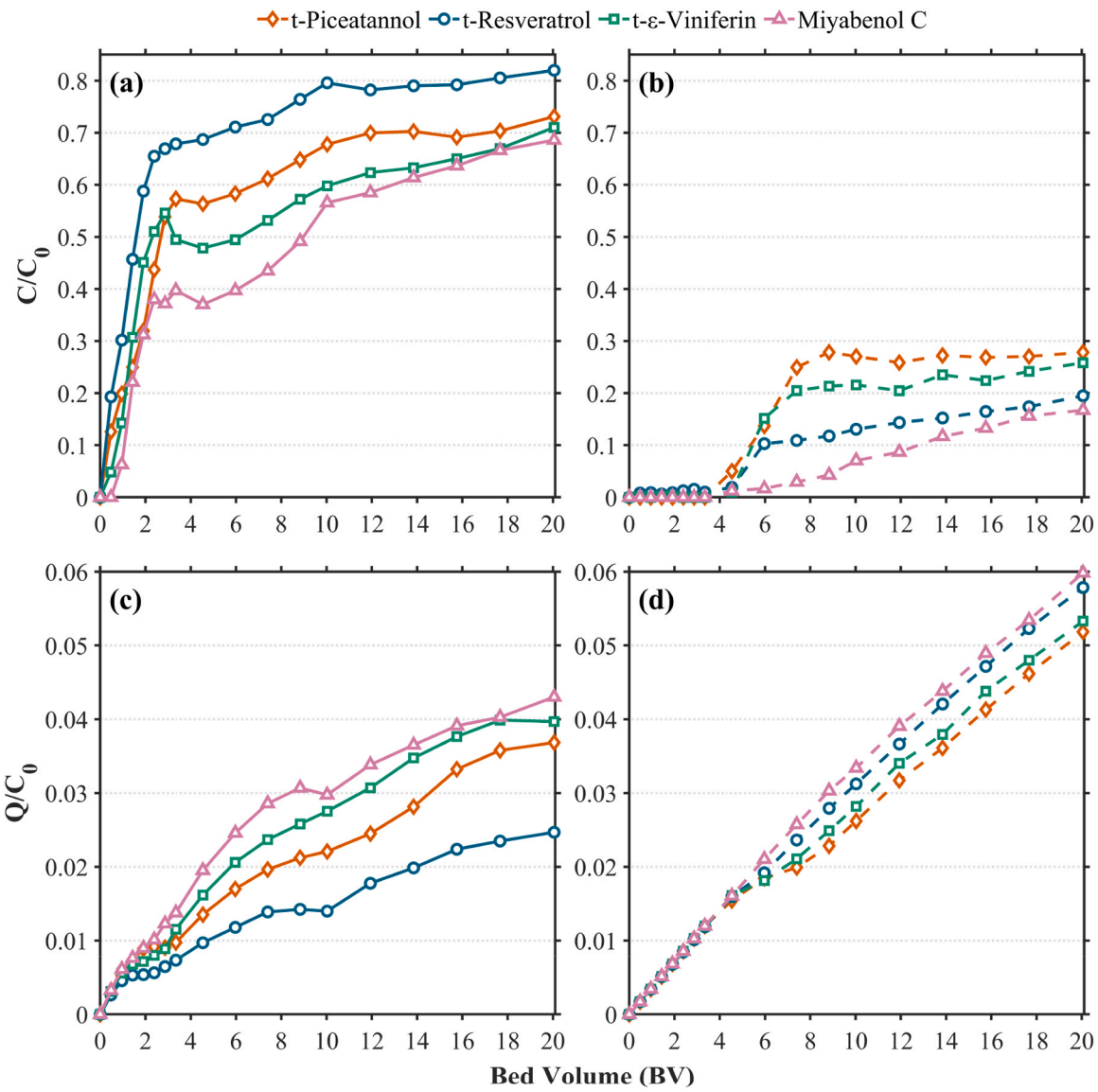

Fig. 9. Dynamic adsorption behaviour of stilbenes, t-piceatannol, t-resveratrol, t-ε-viniferin, and miyabenol C, on poly(BAAPy) and commercial poly(4VP) resin under ethanol-water (1:1, v/v) feed conditions. Panels (a) and (b) show breakthrough curves (C/C_0), while panels (c) and (d) display cumulative uptake (Q/C_0). Data correspond to poly(BAAPy) in (a) and (c), and poly(4VP) in (b) and (d).

corresponding to t-resveratrol, t-ε-viniferin, and miyabenol C. Notably, t-piceatannol was not detected under these conditions, indicating its poor extractability in less polar solvents like ACN.

3.2. *Dynamic adsorption-desorption performance under solvent variation*

To evaluate the selective retention and elution behaviour of stilbene subfamilies under realistic process conditions, dynamic fixed-bed adsorption experiments were conducted using both poly(BAAPy) and poly(4VP) resins. Two solvent systems were tested: acetonitrile (ACN) and ethanol-water (1:1, v/v). Breakthrough curves, cumulative uptake profiles, and adsorption selectivity coefficients were used to assess subfamily-level resolution of monomeric (e.g., t-resveratrol, t-piceatannol) and oligomeric (e.g., t-ε-viniferin, miyabenol C) stilbenes.

3.2.1. *Adsorption-desorption of stilbenes in acetonitrile system*

Under ACN feed conditions, poly(BAAPy) exhibited a highly resolved adsorption hierarchy (Fig. 7-a,c), with t-resveratrol breaking through early, followed by t-ε-viniferin, and miyabenol C. The distinct delays in breakthrough and increasing uptake for the latter two confirm stronger binding affinities toward hydroxylated oligomers. The selectivity coefficient for poly(BAAPy) (Table 3), $S_{Oligomers/Monomers} = 2.00$, quantitatively demonstrates a two-fold preference for oligomeric stilbenes over monomers.

This trend was further supported by the desorption chromatograms in Fig. 8-a. The ACN-based extract eluted from poly(BAAPy) displayed a polarity-responsive release profile: t-resveratrol desorbed early in the water-rich fractions, whereas t-ε-viniferin and miyabenol C progressively eluted with increasing ethanol content, indicating polarity-sensitive elution. This early resveratrol signal is consistent with void-volume displacement/wash-out during the initial 100 % water step, which first flushes the bed before stronger solvent conditions (increasing ethanol) promote elution of the remaining stilbenes.

In contrast, the commercial poly(4VP) resin demonstrated a reversed selectivity pattern (Fig. 7-b,d). t-Resveratrol exhibited the most delayed breakthrough, while both oligomers eluted earlier from the column. The selectivity coefficient for poly(4VP), $S_{Monomers/Oligomers} = 1.19$, confirms a weak preference for monomers over oligomers. Additionally, the adsorption capacity remained low for all analytes, with none achieving full saturation ($C/C_0 \approx 0.3$), likely due to non-specific interactions and

Table 4
Stilbene adsorption selectivity coefficients for oligomeric vs. monomeric stilbenes for poly(BAAPy) and poly(4VP) adsorbents in ethanol-water system (1:1, v/v). Values > 1 indicate preference toward a specific family.

Solvent System	Adsorbent	$S_{Oligomers/Monomers}$
Ethanol-Water (1:1, v/v)	Poly(BAAPy)	1.86
	Poly(4VP) commercial resin	1.01

competitive co-adsorption of extract constituents such as sugars and proteins. Desorption chromatograms of poly(4VP) (Fig. 8-b) further illustrate this limited interaction. Nearly all desorbed species correspond to t-resveratrol in ethanol-rich fractions, with minimal signals for t-ε-viniferin and no detectable miyabenol C, reaffirming the weak adsorption of oligomeric stilbenes on the poly(4VP) resin.

Taken together, these results confirm that poly(BAAPy) enables enhanced subfamily-level resolution under ACN conditions, owing to its

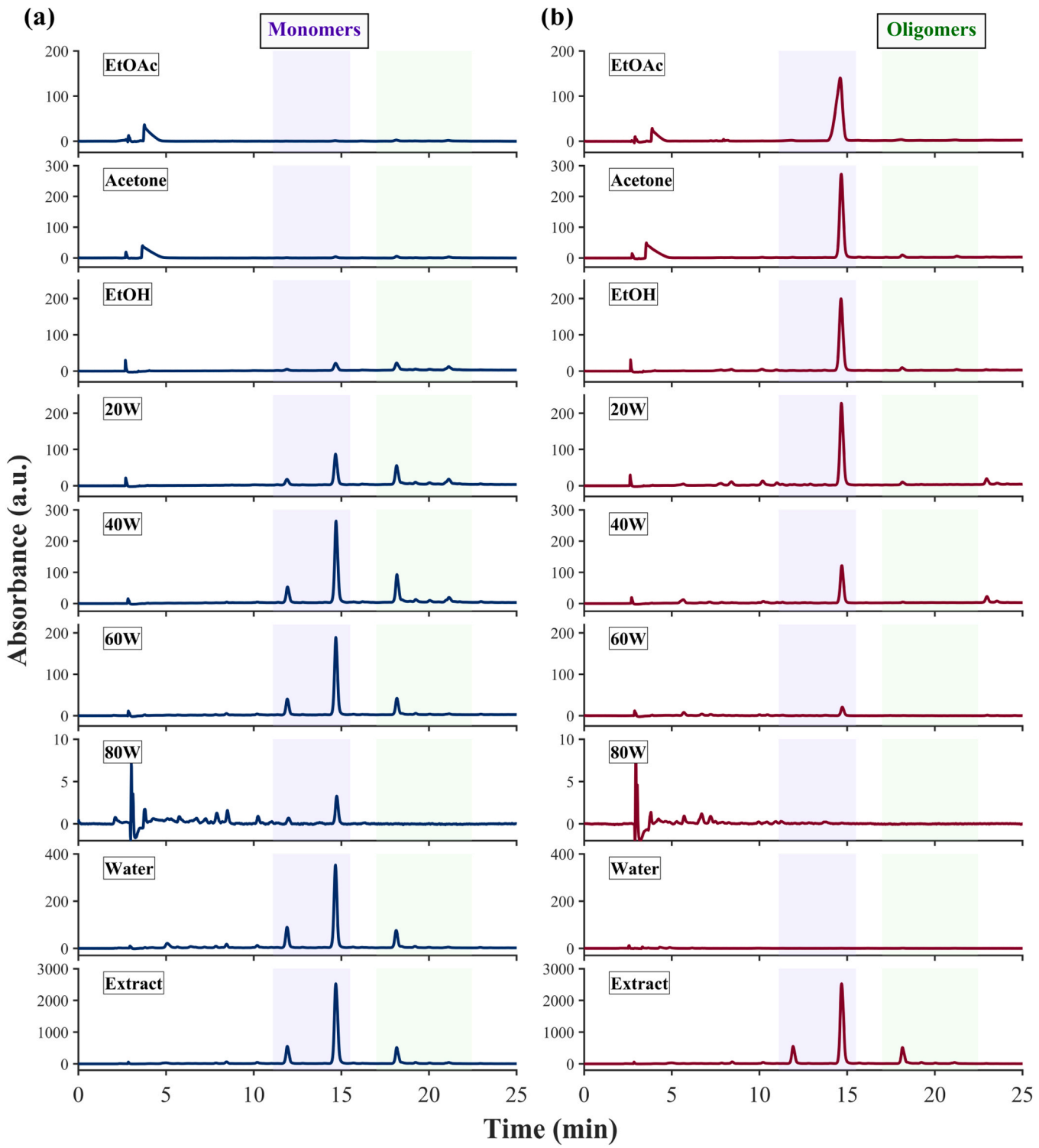

Fig. 10. Desorption chromatograms (λ = 320 nm) of ethanol-water (1:1,v/v) grape cane extract eluted from (a) poly(BAAPy) and (b) poly(4VP) columns. Desorption was performed from water to ethyl acetate (EtOAc) in stepwise polarity gradients. Shaded regions highlight the elution of monomeric versus oligomeric stilbenes.

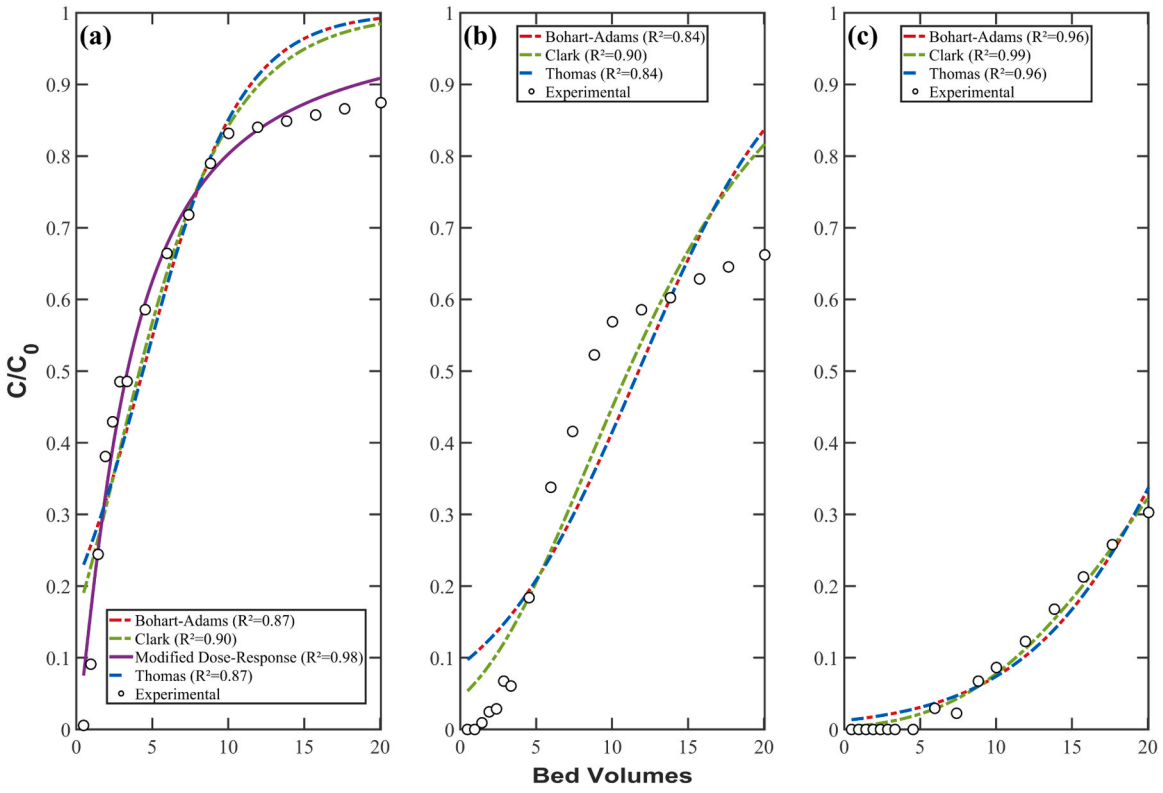

Fig. 11. Breakthrough curve modelling for stilbenes on poly(BAAPy) using ACN-based feed solvent. Panels show: (a) t-resveratrol, (b) t-ε-viniferin, and (c) miyabenol C. Only models achieving $R^2 \geq 0.70$ are displayed. Y-axis is normalized to $C/C_0 = 1$ for comparability across analytes. Due to competitive adsorption using real grape cane extract, analytes do not reach full saturation, resulting in sub-unity plateaus. This reflects inherent inter-analyte competition rather than system limitation.

structural complementarity with hydroxylated oligomers. Its retention mechanism, dominated by multivalent interactions (π–π stacking, H-bonding), distinguishes it from the commercial poly(4VP) resin, which lacks the necessary functionality for selective oligomer recognition. This interpretation is further elaborated in a dedicated section below.

3.2.2. *Adsorption-desorption of stilbenes in ethanol-water system*

To examine whether the observed selectivity trends persist under more polar conditions, the same dynamic adsorption experiments were conducted using ethanol-water (1:1, v/v)-based grape cane extract, which is a green alternative favoured for industrial-scale separations. As expected, both poly(BAAPy) and poly(4VP) exhibited faster breakthroughs (Fig. 9-a,b) and lower cumulative uptakes (Fig. 9-c,d) compared to ACN, indicating overall diminished retention. This decrease in adsorption is attributed to the polar ethanol-water mixture disrupting the interactions with stilbenes.

Despite this reduction, poly(BAAPy) maintained a clear preferential affinity for oligomeric stilbenes, particularly t-ε-viniferin and miyabenol C. This is primarily reflected by their higher cumulative uptakes (Fig. 9-c), while breakthrough onsets are broadly similar for all analytes (Fig. 9-a). The corresponding selectivity coefficient $S_{Oligomers/Monomers}$ remained elevated at 1.86 (Table 4), reinforcing the polymer's capacity for subfamily-level discrimination even under competitive polar conditions. Notably, the slightly lower selectivity in EtOH–water (1.86) compared with ACN (2.00; Table 3) is consistent with stronger solvation and increased hydrogen-bond competition in the more polar medium, which moderates polymer–stilbene interactions and reduces the apparent discrimination under dynamic flow. Despite this, poly(BAAPy) maintains a clear oligomer preference in both solvents, confirming that the selectivity is not solvent-specific.

In contrast, the poly(4VP) resin exhibited tightly clustered breakthrough curves (Fig. 9-b) and minimal differentiation in cumulative uptake across all four analytes (Fig. 9-d), indicating weak selective retention. This behaviour corresponds to a near-unity selectivity coefficient ($S_{Oligomers/Monomers} = 1.01$; Table 4), indicating a lack of preferential retention for either stilbene subclass. These findings suggest that poly(4VP) interactions are governed by general polarity or surface effects rather than specific structural recognition.

Desorption chromatograms (Fig. 10) provide further insight into retention behaviour and analyte elution profiles. On poly(BAAPy), a distinct polarity-dependent desorption pattern was observed: t-resveratrol and t-piceatannol were predominantly recovered in the early water-rich fractions, whereas t-ε-viniferin and miyabenol C eluted gradually with increasing ethanol content. In contrast, desorption from poly(4VP) was dominated by sharp elution of monomeric stilbene t-resveratrol within late fractions, with very weak signals for t-ε-viniferin and no discernible desorption of miyabenol C, again confirming the resin's poor interaction with oligomers.

These results reaffirm poly(BAAPy)'s structural compatibility with complex hydroxylated stilbenes. Even under polar solvent conditions, it enables selective retention and stepwise elution of stilbene subfamilies, underscoring its suitability for scalable subfamily-level fractionation in natural extract processing.

3.3. *Modelling of competitive breakthroughs kinetics*

To investigate the adsorption behaviour of stilbenes on functional polymeric adsorbents, semi-empirical models were used to fit the experimental breakthroughs data presented earlier. The models evaluated include Thomas, Yoon-Nelson, Bohart-Adams, Clark, and the Modified Dose-Response (MDR). Fittings were performed for both poly (BAAPY) and poly(4VP) absorbents under two solvent systems: acetonitrile and ethanol-water (1:1 v/v).

In parallel, a mechanistic model was developed to enable a physics-

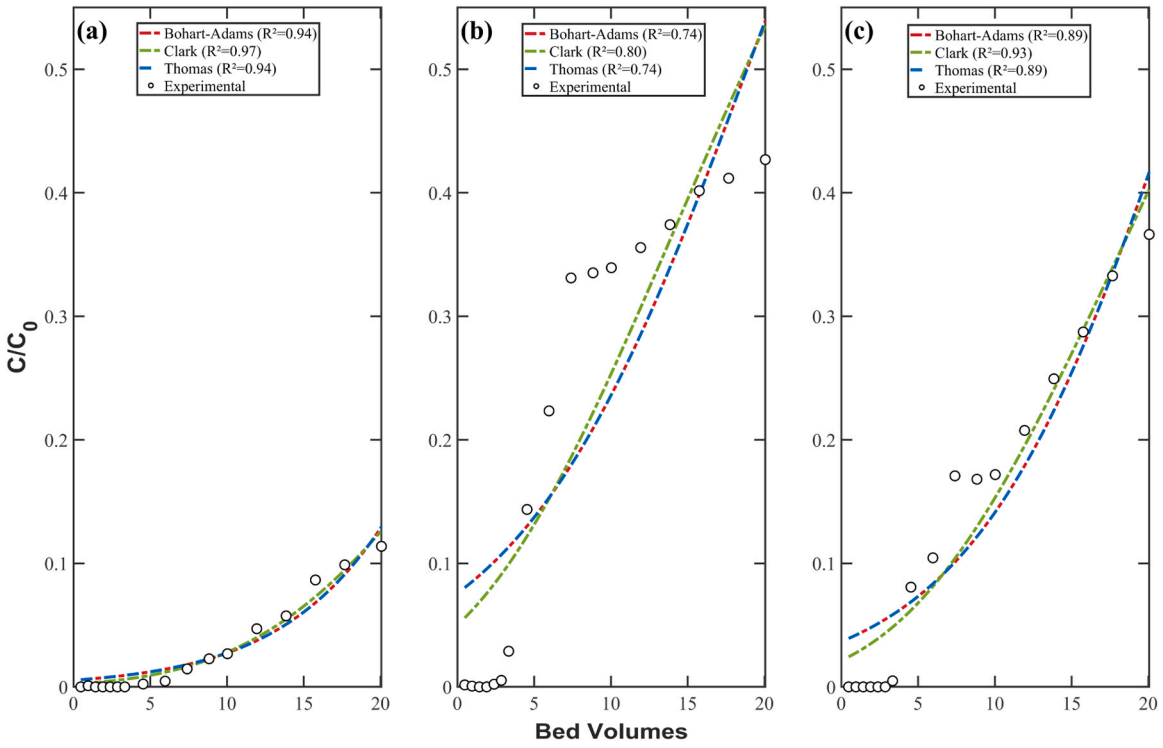

Fig. 12. Breakthrough curve modelling for stilbenes on poly(4VP) using ACN-based feed solvent. Panels show: (a) t-resveratrol, (b) t-ε-viniferin, and (c) miyabenol C. Only models achieving $R^2 \geq 0.70$ are displayed. The Y-axis was standardized to a maximum of 0.55 (C/C_0) across all panels to enhance visual clarity, as breakthrough plateaus remain well below unity due to competitive adsorption from real grape cane extract.

based interpretation of adsorption under dispersive flow and non-saturating conditions (see Supplementary Information, Section S6). This model incorporates axial dispersion, single-site Langmuir equilibrium, and intraparticle mass transfer approximated by the Linear Driving Force (LDF) model. While the detailed mechanistic model supports a deeper kinetic understanding, the present section focuses on the comparative fitting performance and applicability of the semi-empirical models for breakthrough data interpretation.

3.3.1. *Model performance under acetonitrile feed conditions*

Under ACN feed conditions, breakthrough profiles were sharper and more symmetric for both adsorbents, particularly for oligomeric stilbenes. For poly(BAAPy) (Fig. 11), Clark model consistently provided the best agreement for t-ε-viniferin ($R^2 = 0.90$, RMSE = 0.08) and miyabenol C ($R^2 = 0.99$, RMSE = 0.01), followed closely by Bohart-Adams and Thomas models. The MDR model excelled for monomeric analytes such as t-resveratrol ($R^2 = 0.98$; RMSE = 0.03).

For poly(4VP), while the breakthrough profiles were generally flatter and less resolved (Fig. 12), acceptable fits were still achieved using Clark, Bohart-Adams, and Thomas models for t-resveratrol and miyabenol C ($R^2 \geq 0.90$). However, predictive accuracy deteriorated for t-ε-viniferin, where early elution and dispersion led to lower quality fits (e.g., $R^2 = 0.80$, RMSE = 0.08). The Yoon-Nelson model failed consistently across all analytes (e.g., $R^2 = -2.35$ for t-ε-viniferin; Supporting Information S5), due to its rigid symmetry assumptions, which do not hold in complex extract matrices [37].

3.3.2. *Model trends under aqueous ethanol conditions*

In ethanol-water systems, overall model accuracy declined relative to ACN, driven by broader breakthrough fronts and reduced saturation levels. For poly(BAAPy) (Fig. 13), MDR model maintained strong predictive performance ($R^2 \geq 0.89$) across all analytes, reflecting its robustness under lower plateau conditions. The Clark model underperformed slightly but still provided acceptable fits for t-piceatannol and miyabenol C ($R^2 > 0.70$).

For poly(4VP) (Fig. 14), the Clark model emerged as the most consistent across analytes, achieving acceptable fits ($R^2 \geq 0.70$) for t-resveratrol and t-ε-viniferin, and a strong fit for miyabenol C ($R^2 = 0.92$). The Thomas and Bohart-Adams models also produced satisfactory fits for miyabenol C ($R^2 = 0.92$). In contrast, MDR and Yoon-Nelson models underperformed in ethanol-water system with negative R^2 values, illustrating the challenge of simulating poorly retained analytes under polar solvent conditions.

3.3.3. *Model suitability and limitations*

Comparative evaluation of kinetic models across adsorbents, solvents, and stilbene subclasses revealed that no single semi-empirical model consistently outperformed others. Under acetonitrile feed conditions, where breakthrough curves were sharper and more symmetric, models such as Thomas, Clark, and Bohart-Adams provided excellent fits. For example, the Clark model achieved $R^2 = 0.99$ for miyabenol C on poly(BAAPy). -In contrast, the ethanol-water system produced broader and more gradual breakthroughs, reducing model fidelity for compounds exhibiting tailing, weak binding, or asymmetric behaviour.

These limitations arise from the intrinsic simplifications of semi-empirical models, which often fail to account for multicomponent phenomena such as competitive sorption, matrix-induced interference, and partial saturation, which are features commonly observed in complex natural extracts [38,39].

To address this, a mechanistic model incorporating axial dispersion, film resistance, and Langmuir-type adsorption equilibrium was employed (see Section 6, Supporting Information). While this model provides a physically grounded view of sorption dynamics, its application to natural extracts remains challenging. Incomplete saturation, especially in early breakthrough or plateaued profiles, complicates parameter identifiability. This was further supported by the fitted parameters in Table S3 (with fitting curves shown in Figures S8-S11), which showed solvent and adsorbent dependent variations in both

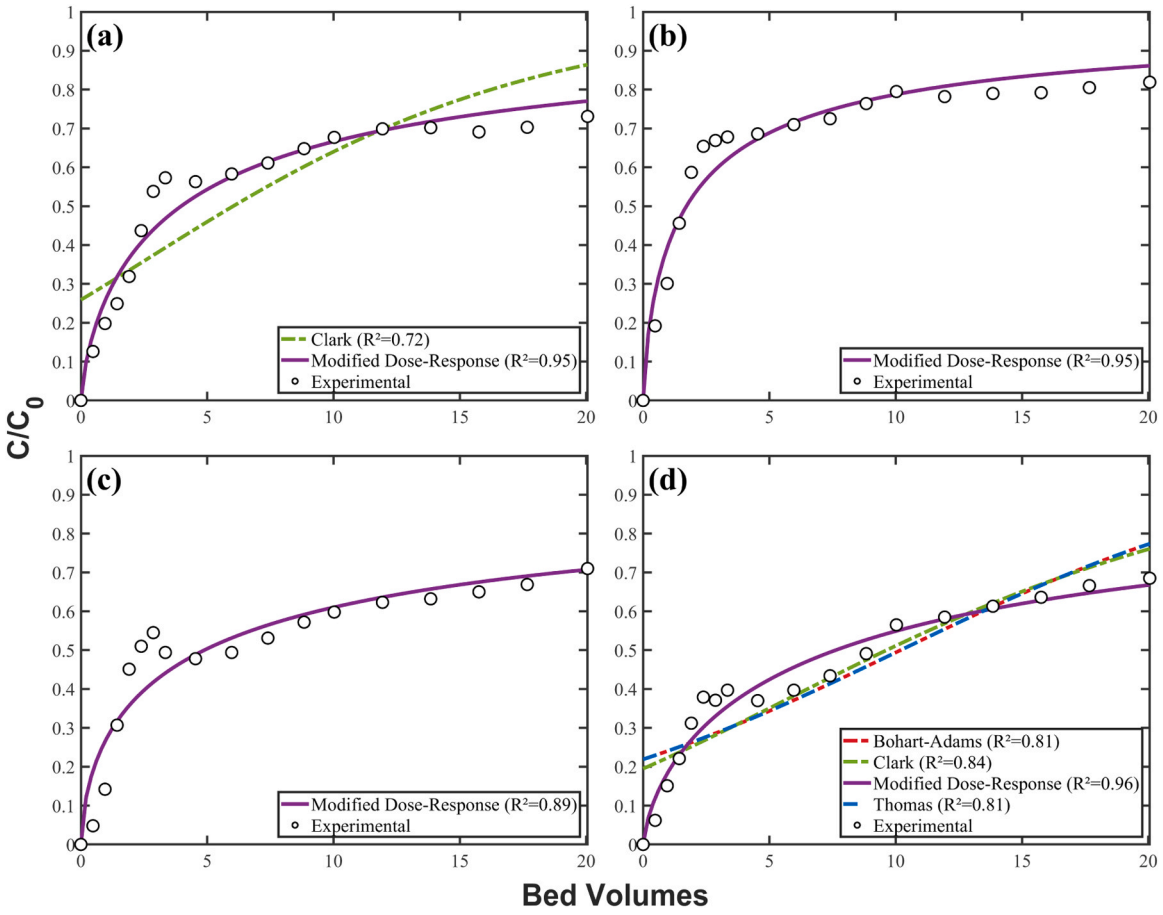

Fig. 13. Breakthrough curve modelling for stilbenes on poly(BAAPy) using EtOH-W (1:1, v/v) as extract feed solvent. Panels show: (a) t-piceatannol, (b) t-resveratrol, (c) t-ε-viniferin, and (d) miyabenol C. Only models achieving $R^2 \geq 0.70$ are displayed.

adsorption capacities (q_{max}) and mass transfer coefficients (K_{LDF}), highlighting the sensitivity of mechanistic fitting to operating conditions and extract complexity. Poly(BAAPy) consistently exhibited higher q_{max} values than poly(4VP), and ethanol-water (1:1) system generally enhanced kinetic parameters (K_{LDF}) across all compounds. These trends suggest a compound-specific interplay between polymer chemistry, solvent polarity, and stilbene structure.

Together, these results validate the role of the mechanistic model as a complementary tool to semi-empirical approaches. While the latter enable efficient comparison and initial screening, mechanistic fitting adds interpretive power, particularly under low-saturation conditions, or when probing structure-selective interactions between adsorbents and target solutes.

3.4. Mechanistic basis for stilbene retention on functional polymer adsorbents

The divergent selectivity profiles of poly(BAAPy) and poly(4VP) resins, evident in both breakthrough and desorption data, stem from their intrinsic chemical architectures. Poly(4VP) is composed of repeating pyridyl monomers, whereas poly(BAAPy) incorporates both amide and pyridine functionalities via 2,6-bis(acrylamido)pyridine units. These structural differences dictate the nature and strength of the interactions formed with hydroxylated stilbenes.

In addition to surface chemistry, the physical morphology of the adsorbent can influence wetting and mass transfer to binding sites under dynamic flow. SEM micrographs of poly(BAAPy) (Fig. 15) show irregular, fractured particles with a rough, micro-textured surface across multiple length scales (agglomeration of precipitation polymerization nucleus with size < 1 μm). Such a heterogeneous, textured surface is consistent with good solvent access and short diffusion distances to near-surface functional domains, which supports efficient uptake under the fixed-bed conditions used here.

Measurement of the specific surface area and pore volume of the produced poly(BAAPy) adsorbent particles reveals values of 214.8 m^2/g and 0.15 cm^3 /g, respectively. The BJH adsorption cumulative surface area of pores with diameter between 17 and 3000 Å was measured to be 147 m^2/g. These measurements indicate a much higher surface area and pore volume than the Reillex® 402 adsorbent (with a measured surface area of 0.5 m^2/g and an estimated pore volume of 0.000463 cm^3/g, based on experimental data in the SI file). This difference is due to the microporous structure of the 4VP/DVB 98/2 gel-type resin rather than a macroporous polymer network. The surface area properties of the novel poly(BAAPy) adsorbent reported here are included in the range of other commercial polymer adsorbents (e.g., 140–160 m^2/g for the acrylic ester DAX8 adsorbent and 750 m^2/g for the polystyrene divinylbenzene XAD4 resin), but much lower than usual values for activated carbon adsorbents (>1000 m^2/g). Overall, the good binding capacity of the 4VP material toward polyphenols, which was previously demonstrated [22–24,26–28], and the capacity of the poly(BAAPy) material for targeting oligomeric stilbenes are consequences of the high functional content of these polymer networks with respect to pyridyl and amide-pyridine groups, respectively.

Consistent with this accessible particle surface (Fig. 15), poly (BAAPy) exhibits a high density of H-bond donors/acceptors and aromatic groups, offering a dense interaction network with polyphenols [28]. Its extended architecture facilitates cooperative multivalent binding, especially with oligomeric stilbenes such as t-ε-viniferin and

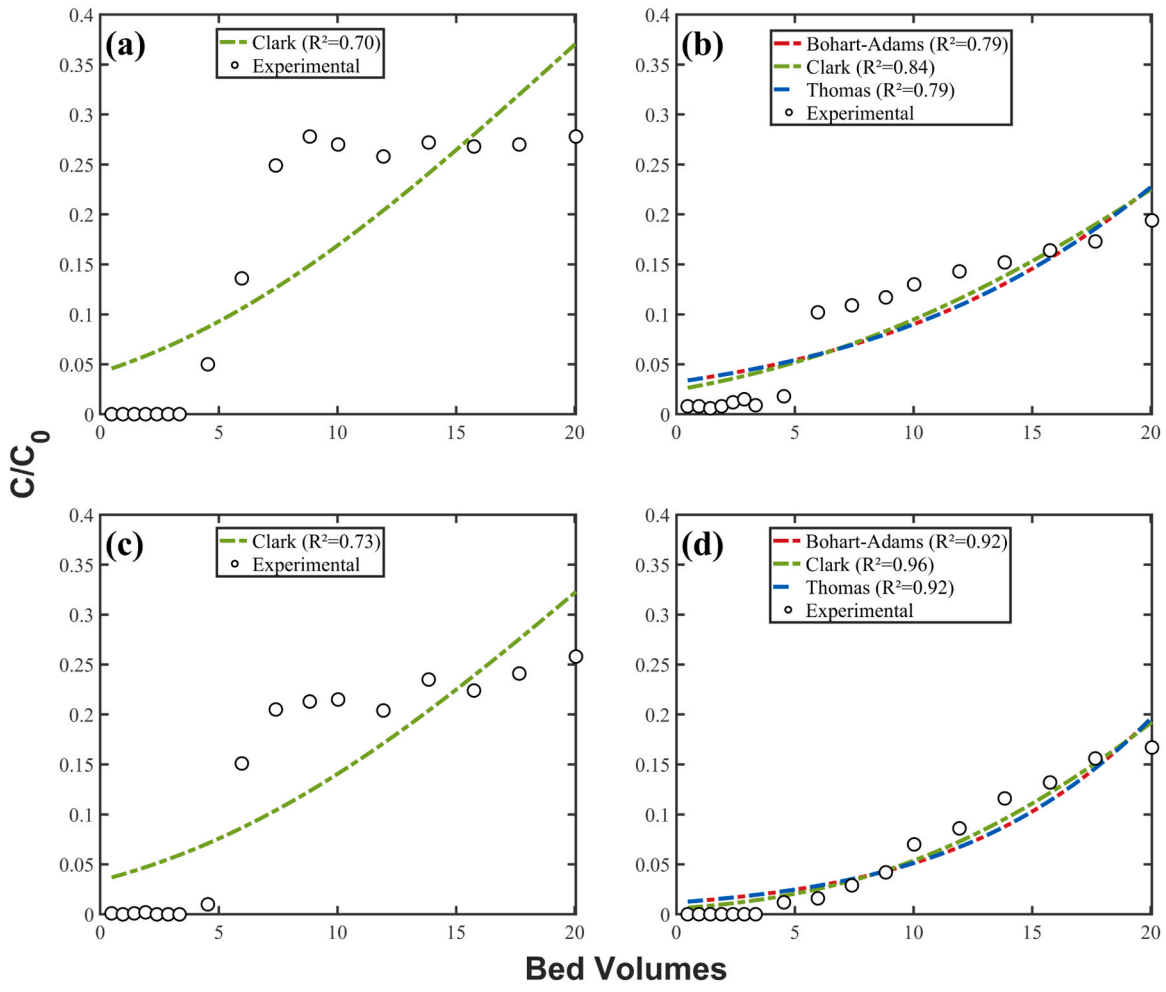

Fig. 14. Breakthrough curve modelling for stilbenes on poly(4VP) using EtOH-W (1:1, v/v) as extract feed solvent. Panels show: (a) t-piceatannol, (b) t-resveratrol, (c) t-ε-viniferin, and (d) miyabenol C. Only models achieving $R^2 \geq 0.70$ are displayed.

miyabenol C, which possess numerous hydroxyl and aromatic moieties. As illustrated in Fig. 16-a, these compounds engage in hydrogen bonding, N-H···π, and π–π stacking, resulting in pronounced retention and delayed breakthroughs of oligomeric stilbenes.

By contrast, monomeric stilbenes like t-resveratrol and t-piceatannol possess fewer hydroxyl groups and aromatic rings, leading to weaker interactions with poly(BAAPy). This limited interaction is consistent with the breakthrough profiles observed in both ACN and ethanol-water systems.

Beyond specific binding modes, non-specific interaction such as hydrophobic effects and solvent-mediated forces, also contribute to overall retention behaviour. In polar solvent systems like ethanol-water, hydrophobic interactions may become more prominent, altering the adsorption profile of stilbenes through changes in solvation and partitioning behaviour. Additionally, entropic factors, such as conformational rearrangement of flexible molecules, likely influence the overall affinity of the analytes for the polymer matrix [40]. These broader physicochemical contributions are particularly relevant in multicomponent systems, where analyte-matrix and analyte-solvent interactions may compete with polymer binding, further shaping breakthrough trends.

Regarding the poly(4VP) adsorbent, its network has fewer interactive sites than poly(BAAPy). In fact, each repeating unit of 4VP contains a single pyridyl group that can engage in hydrogen bonding via its nitrogen. As depicted in Fig. 16-b, the reduced complexity of poly(4VP) matrix limits the formation of stable complexes with larger oligomers. This mechanistic shortcoming aligns with the lower retention and poor selectivity toward t-ε-viniferin and miyabenol C across all tested conditions.

The contrast between the polymers is quantitatively captured by the selectivity coefficients: poly(BAAPy) achieves $S_{Oligomer/Monomers}$ of 2.00 in ACN and 1.86 in ethanol-water, indicating a strong preference for oligomeric stilbenes. In contrast, poly(4VP) shows weak or negligible discrimination for any stilbene subfamily ($S_{Oligomer/Monomers}$ of 0.84 in ACN and 1.01 in ethanol-water), alongside lower saturation levels ($C/C_0 \approx 0.3$), likely due to co-adsorption of matrix solutes like tannins and sugars.

Altogether, the enhanced performance of poly(BAAPy) is attributed to its higher functional group density and favourable topological arrangement, enabling structurally complementary, multivalent interactions. These mechanistic interpretations are supported by literature on polyphenol adsorption, where pyridine- or imidazole-functionalized resins enhance selectivity via hydrogen-bonding networks [41]. Notably, selectivity often scales with the number of H-bonding groups on the polymer, reinforcing the importance of multivalent binding for differentiating phenolic substructures [28,42].

Importantly, this mechanistic interpretation is grounded in the experimental outputs: the reproducible oligomer/monomer retention hierarchy, solvent-dependent shifts in breakthrough/desorption profiles, and the consistent contrast to the poly(4VP) control quantified by the selectivity coefficients.

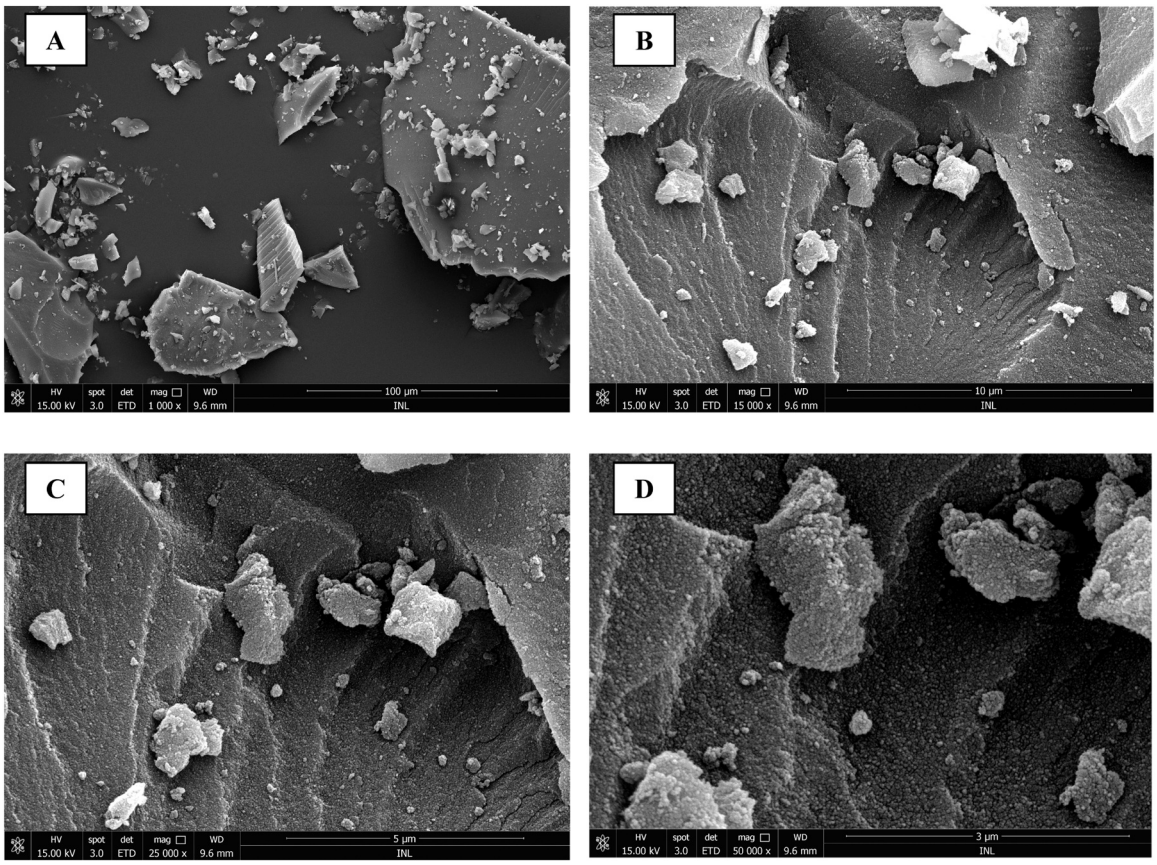

Fig. 15. SEM micrographs of poly(BAAPy) showing particle morphology at increasing magnification: (A) overview of fractured particles (scale bar: 100 µm); (B) surface features on particle fragments (10 µm); (C) higher-magnification view of micro-textured surfaces (5 µm); (D) fine surface texture at the sub-micron scale (3 µm). Magnification ranged from 1000 × to 50000 × as indicated.

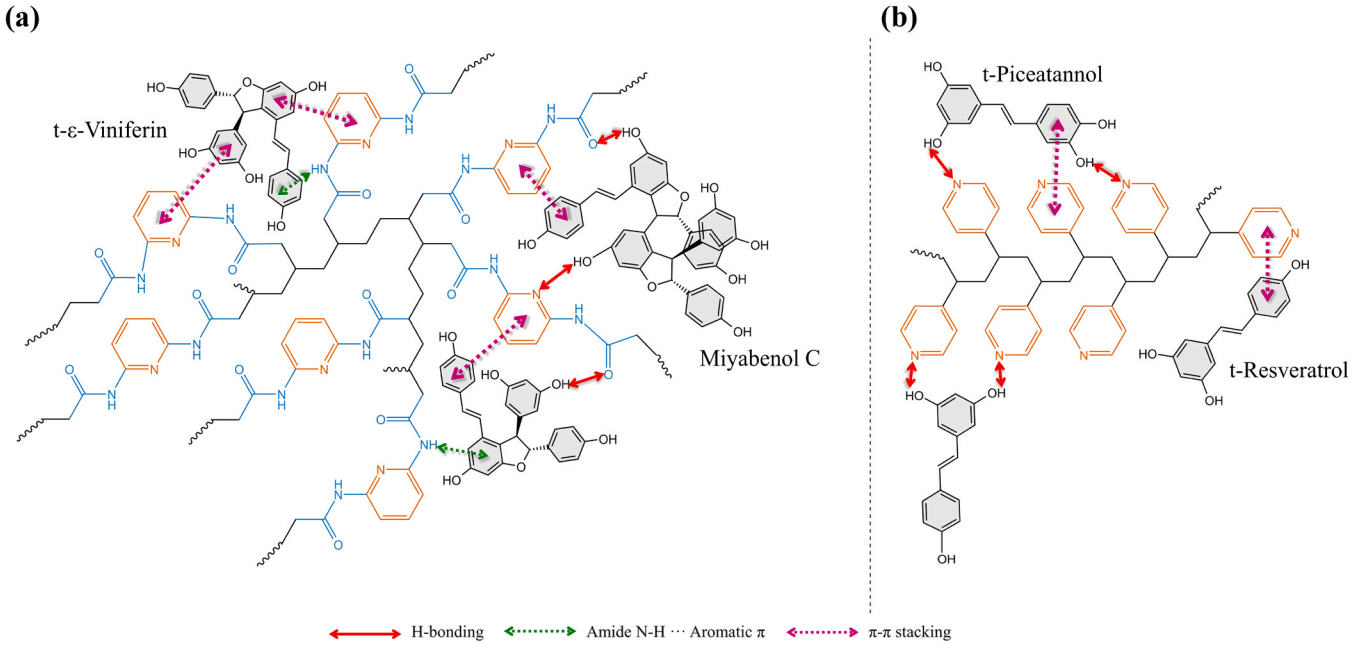

Fig. 16. Conceptual schematic of plausible interaction mechanisms proposed to rationalize the adsorption selectivity trends observed for the two adsorbents.(a) Poly (BAAPy) retains stilbene oligomers via multivalent π-π stacking, H-bonding, and NH-aromatic π interactions. (b) Poly(4VP) engages in π-π interactions and pyridyl-based hydrogen bonding, favouring the retention of monomeric stilbenes. Interaction types are color-coded: π-π stacking (magenta), H-bonding (red), and NH-aromatic π contacts (green). Each compound is labelled once, despite multiple appearances, to show distinct binding modes.

Table 5
Stilbene adsorption selectivity coefficients for oligomeric vs. monomeric stilbenes for poly(BAAPy) and poly(4VP) adsorbents in ethanol-water mixture (1:1, v/v). Values > 1 indicate preference toward a specific family.

Solvent System	Adsorbent	$S_{Oligomers/Monomers}$
Ethanol-Water (1:1, v/v)	Poly(BAAPy)	1.30
	Poly(4VP) commercial resin	1.01

3.5. Fractionation of stilbene subfamilies in a closed-loop dynamic adsorption system

To demonstrate the practical potential of poly(BAAPy) for scalable phytochemical recovery, a closed-loop dynamic adsorption system was implemented using crude grape cane extract in ethanol-water (1:1, v/v) as feed (scheme depicted in Fig. 2). This green solvent system is food-grade, biodegradable, and more sustainable than acetonitrile, making it suitable for scalable nutraceutical applications. The system emulates realistic processing conditions by continuously recirculating the solution through a packed column until dynamic equilibrium is reached, followed by stepwise desorption with eluents of increasing polarity [43, 44]. Both synthesized poly(BAAPy) and commercial poly(4VP) resins were evaluated under identical dynamic flow conditions (constant empty-bed contact time), enabling direct comparison of their adsorption and fractionation performance toward monomeric and oligomeric stilbenes. Table 5 summarizes the selectivity observed during adsorption. Poly(BAAPy) demonstrated a clear preferential affinity for oligomeric stilbenes ($S_{Oligomers/Monomers}$ = 1.30), whereas poly(4VP) displayed a near-unity selectivity (1.01), indicating non-selective adsorption. This difference highlights the stronger interaction of poly(BAAPy) with higher-order stilbenes due to multidentate binding mechanisms. The lower $S_{Oligomers/Monomers}$ in closed-loop mode (Table 5) compared with open-loop operation (Table 4) is expected because recirculation causes the feed composition and concentrations to evolve during adsorption and the bed to progressively load, which reduces the apparent selectivity coefficient derived from breakthrough behaviour.

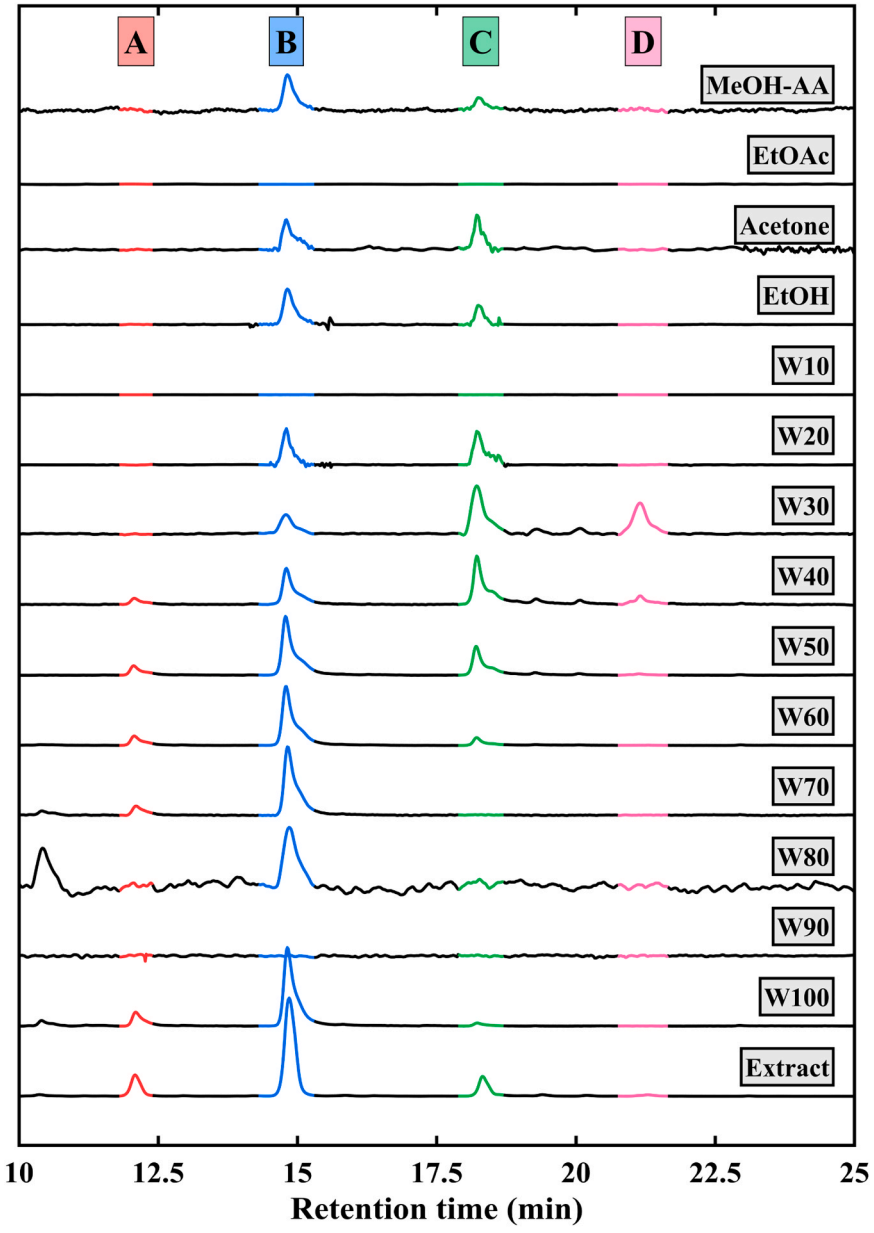

Fig. 17. HPLC-DAD chromatograms (λ = 320 nm) of eluted fractions from poly(BAAPy) after closed-loop dynamic adsorption. The desorption sequence ranges from 100 % water (W100) to methanol-acetic acid (9:1, v/v; MeOH-AA).

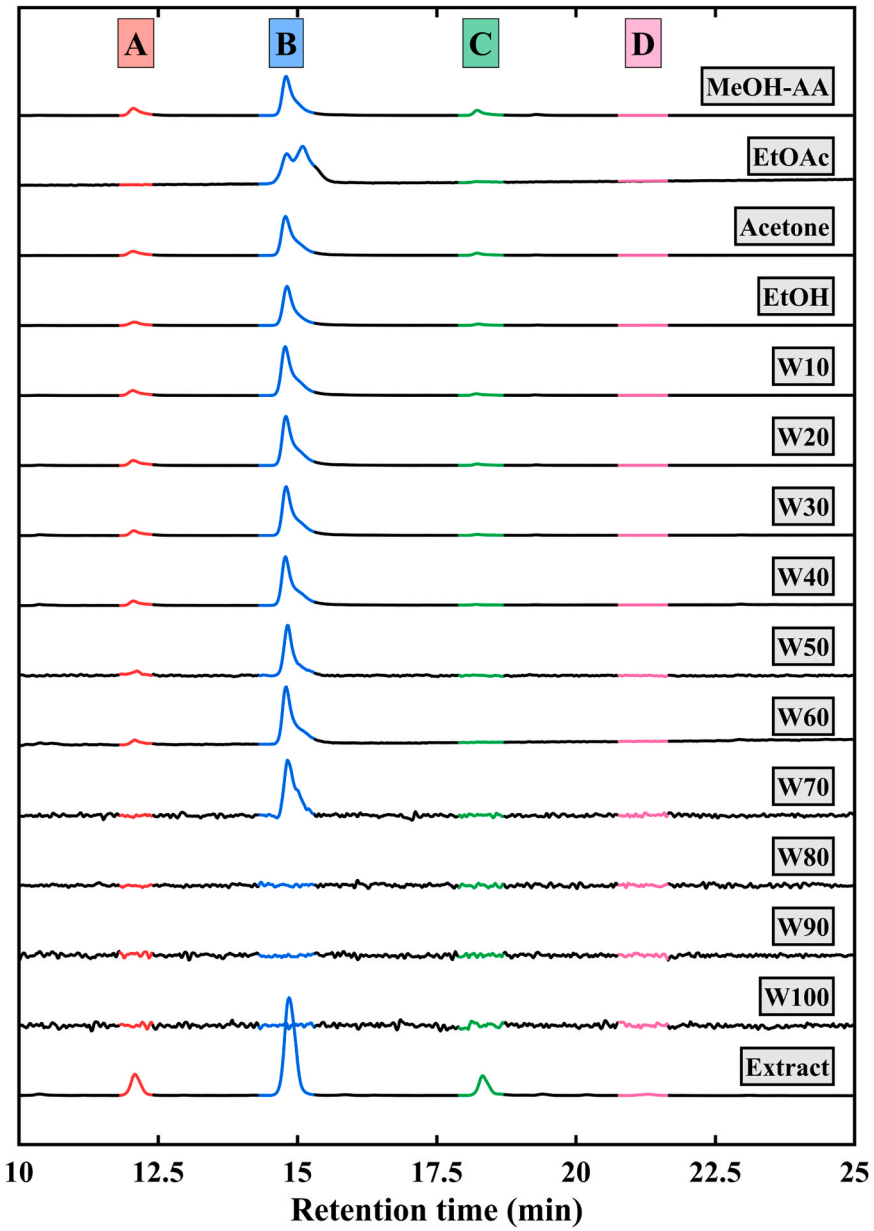

Fig. 18. HPLC-DAD chromatograms (λ = 320 nm) of eluted fractions from poly(4VP) after closed-loop dynamic adsorption. The desorption sequence ranges from 100 % water (W100) to methanol-acetic acid (9:1, v/v; MeOH-AA).

Figs. 17 and 18 showcase the sequential HPLC-DAD chromatograms obtained during closed-loop dynamic elution from poly(BAAPy) and poly(4VP), respectively. On poly(BAAPy), the chromatographic profile reveals clear subfamily-resolved retention behaviour. Monomeric stilbenes, t-piceatannol (peak A) and t-resveratrol (peak B), eluted predominantly in early aqueous fractions (W100–W50), indicating weaker interactions with the polymer. In contrast, oligomeric stilbenes, t-ε-viniferin (peak C) and miyabenol C (peak D), eluted progressively in later ethanol-rich and organic fractions (W40-acetone), reflecting stronger and delayed desorption. This gradient-dependent release pattern underscores poly(BAAPy)'s multivalent binding capability and structural compatibility with hydroxylated oligomers. Conversely, elution from poly(4VP) remained uniform across all fractions. Peaks A and B (monomers) appeared with similar intensities throughout the sequence, regardless of solvent polarity. Peaks C and D, corresponding to oligomeric stilbenes, were barely detectable or entirely absent in the collected fractions, indicating minimal recovery of oligomers from poly (4VP) under these conditions (i.e., oligomers largely pass through during loading and/or are not efficiently eluted). This flat elution pattern highlights poly(4VP)'s limited capacity for subfamily differentiation and supports its lack of multidentate interaction sites necessary for selective oligomer capture.

Fig. 19 provides a quantitative breakdown of stilbene subfamily distributions across the elution fractions, capturing the distinct fractionation behaviour of poly(BAAPy) and poly(4VP). In Fig. 19-a, poly (BAAPy) demonstrated a marked enrichment of oligomeric stilbenes: their proportion rose sharply from ~25 % in the initial feed (indicated by the red star) to nearly 90 % by fraction W30. This shift reflects progressive elution of higher-order stilbenes in later, increasingly organic fractions, consistent with stronger retention through multivalent interactions. In contrast, the monomeric subfamily (marked by the blue star) dominated early aqueous fractions. Conversely, Fig. 19-b shows that poly(4VP) failed to effectuate any significant subfamily resolution: the monomer-to-oligomer ratios remained nearly constant across all fractions. This behaviour reflects its weak structural complementarity and minimal interaction with hydroxyl-rich oligomers. Fig. 19-c

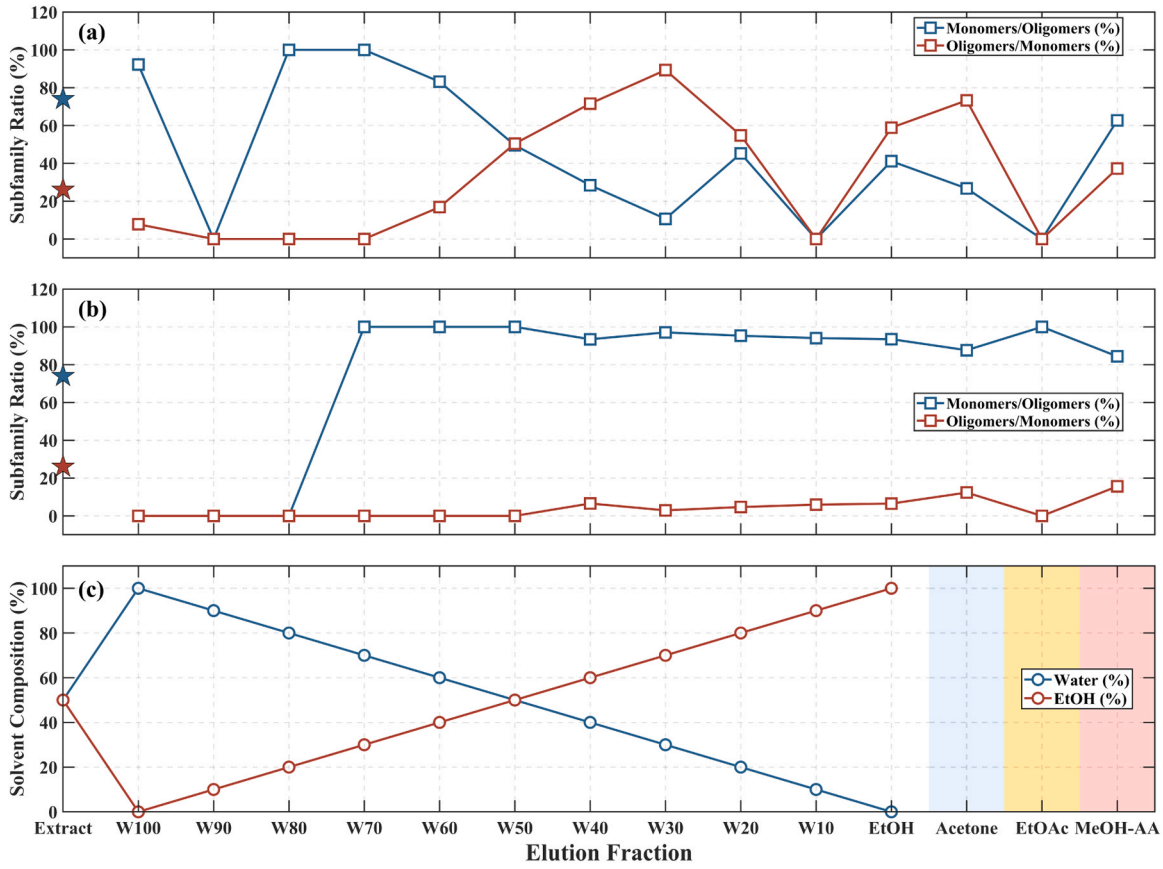

Fig. 19. Stilbene subfamily composition across sequential elution fractions. for poly(BAAPy) and poly(4VP) adsorbents. (a) Subfamily compositions for poly(BAAPy): monomers-to-oligomers (%) and oligomers-to-monomers (%) across gradient elution steps. (b) Subfamily compositions for commercial poly(4VP) (Reillex® 402) under the same conditions. (c) Solvent composition (% v/v) for each fraction, showing water and ethanol variation from W100 (100 % water) to EtOH (100 % ethanol), followed by pure organic solvents: acetone, ethyl acetate (EtOAc), and methanol-acetic acid (9:1, v/v; MeOH-AA). Red and blue stars indicate the subfamily compositions in the original extract (EtOH-water, 1:1, v/v).

contextualizes these trends by overlaying the gradual solvent transition from fully aqueous (W100) to fully organic (EtOH, acetone, EtOAc and MeOH-AA). The progressive increase in ethanol content strongly correlates with the delayed elution of oligomers on poly(BAAPy), underscoring the polarity-driven nature of their desorption.

Fig. 20 further reinforces these findings through enrichment factor heatmaps. Poly(BAAPy) (panel a) displayed robust and consistent enrichment of oligomeric stilbenes across multiple fractions, reaching an $E_{Oligomers/Monomers}$ of 3.43 in W30 and maintaining values above 2.0 through W40 to acetone fractions. In sharp contrast, poly(4VP) (panel b) displayed oligomer depletion across all fractions ($E_{Oligomers/Monomers} \approx 0.25$), alongside slight monomer enrichment ($E_{Monomers/Oligomers} \approx 1.35$).

For contextual comparison, Table 6 provides an overview of representative strategies used to achieve stilbene family-/subfamily-level fractionation from plant-derived matrices (i.e., separation between monomers and oligomers and/or resolution within monomeric and oligomeric subclasses). Most of these approaches rely on multi-step workflows such as high-speed counter-current chromatography (HSCCC), centrifugal partition chromatography (CPC), medium-pressure liquid chromatography (MPLC), or gradient-based reversed-phase HPLC, often require system-specific optimization to resolve structurally similar stilbenes, whether across families (monomers vs oligomers) or within each family (e.g., different monomers or oligomeric subclasses). In several cases (e.g., seed kernel, grape shoots), complex elution modes or partial separations are reported, indicating persistent challenges in handling structurally similar stilbene subclasses. In this context, the poly(BAAPy)-based fixed-bed dynamic adsorption system delivers a compelling alternative. While still reliant on a gradual solvent gradient (Fig. 19-c), it achieves progressive, subfamily-selective elution within a single adsorption-desorption cycle. Importantly, the use of aqueous ethanol facilitates polarity-driven elution in a safer, cost-effective, and industry-compatible solvent system, avoiding the use of more hazardous solvents like acetonitrile—without compromising oligomeric stilbene enrichment. Notably, poly(BAAPy) achieves enrichment factors exceeding 3.4 for oligomeric stilbenes (Fig. 20) and enables their elution with ~90 % subfamily purity in the W30 fraction, outperforming several multi-step or solvent-intensive techniques in Table 6. Importantly, the total stilbene recovery was 75.08 % for poly (BAAPy) and 78.92 % for poly(4VP), confirming that the enhanced selectivity of poly(BAAPy) does not compromise overall extraction efficiency. Unlike traditional strategies requiring multiple chromatographic passes (e.g., recycling HPLC, MPLC), this system offers operational simplicity, minimal solvent use, and a scalable design suitable for natural extract processing.

The adsorption/desorption behaviour reported here is governed by reversible, non-covalent interactions, which makes the process inherently compatible with regeneration by solvent switching. Accordingly, the stepwise polarity gradient used for desorption (aqueous ethanol followed by organic eluents) also functions as an in-column cleaning/regeneration step to remove retained stilbenes and recondition the bed prior to subsequent operation. Poly(BAAPy) is employed as an insoluble, crosslinked particulate packed in a frit-retained fixed bed, which is the standard configuration to ensure particulate containment during dynamic operation. While systematic multi-cycle performance tracking was beyond the scope of this study, the robust solvent-driven recovery of

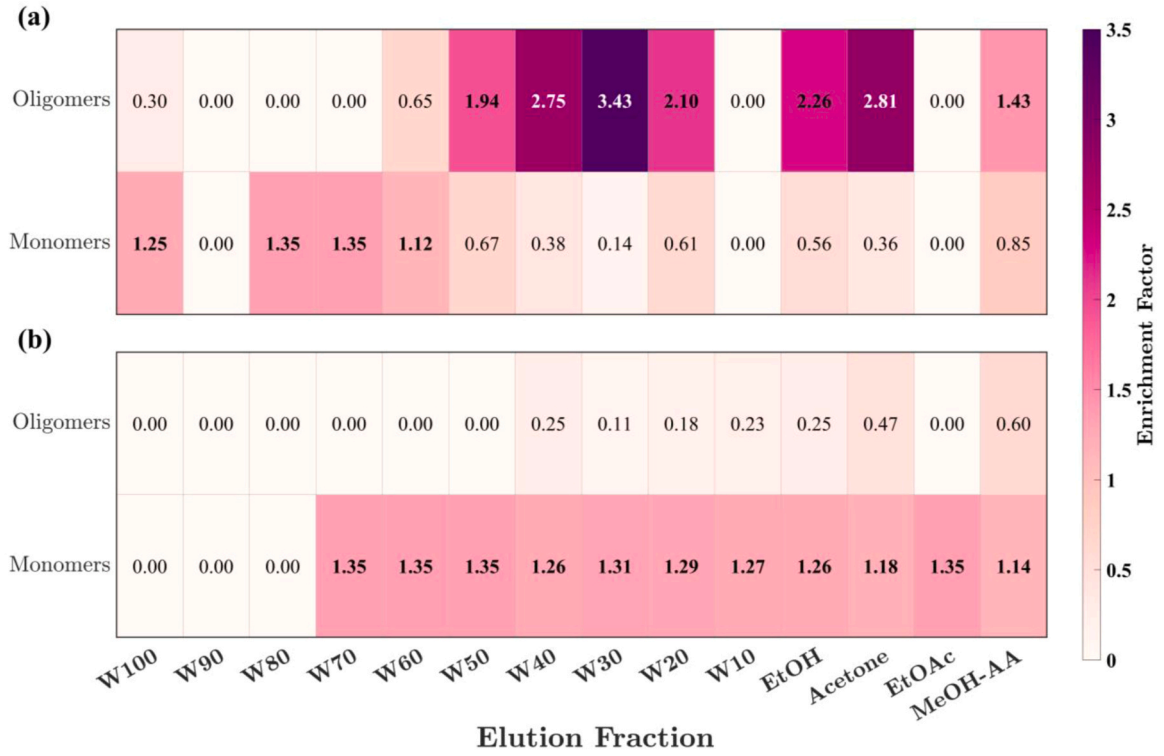

Fig. 20. Enrichment factors for monomeric and oligomeric stilbenes across sequential elution fractions for (a) poly(BAAPy) and (b) commercial poly(4VP). Enrichment factors were calculated relative to the compositions of the original extract (EtOH-water, 1:1, v/v).

retained stilbenes supports the practical feasibility of repeated adsorption–desorption use in fixed-bed operation.

The bio-functional advantage of targeting oligomeric stilbenes such as t-ε-viniferin and miyabenol C further elevates this method's relevance. These compounds exhibit enhanced bioactivity compared to monomeric analogues [45,46]. In fact, resveratrol oligomers have been shown to outperform the monomer t-resveratrol in both DPPH and lipid oxidation assays [46]. In addition, oligomers like t-ε-viniferin, have been shown to inhibit *Plasmopara viticola* sporulation, offering a green fungicide alternative for agricultural applications [47].

Overall, poly(BAAPy) emerges as a highly effective material for scalable, selective fractionation of structurally similar yet functionally distinct stilbenes, highlighting its significant potential for industrial phytochemical recovery processes. The adoption of an ethanol-water solvent system further enhances this potential by supporting clean-label extraction practices and minimizing environmental impact, consistent with the growing demand for eco-conscious and food-grade processing in nutraceutical and pharmaceutical industries.

4. Conclusions

Compositional screening across Portuguese grape cane cultivars confirmed the consistent presence of diverse bioactive stilbenes, highlighting grape cane waste as a sustainable and underutilized feedstock for high-value compound recovery. This study demonstrated that poly (BAAPy), a novel amide–pyridine functional polymer, enables subfamily-selective retention and fractionation of oligomeric stilbenes under dynamic fixed-bed conditions, outperforming a commercial poly (4VP) resin in both ethanol–water and acetonitrile systems.

Breakthrough and desorption analyses revealed a clear preference of poly(BAAPy) for oligomeric stilbenes (e.g., trans-ε-viniferin, miyabenol C), driven by multivalent hydrogen bonding and π–π stacking interactions. Kinetic modelling using both empirical and mechanistic approaches validated these selectivity patterns and provided quantitative insights into adsorption dynamics.

Under closed-loop dynamic operation, poly(BAAPy) enabled polarity-responsive elution, achieving 75 % total stilbene recovery, subfamily purities $\geq$ 90 %, and enrichment factors exceeding 3.4 in a single desorption cycle. These outcomes demonstrate efficient family-level fractionation and oligomer enrichment in a single adsorption–desorption cycle. The resulting enriched fractions can be used directly where mixture enrichment is sufficient, or used as an upstream pre-concentration and matrix-simplification step prior to HSCCC/CPC/preparative HPLC when single-compound purity is required.

Although this study establishes effective subfamily-level fractionation and oligomer enrichment under dynamic fixed-bed operation, several complementary aspects remain beyond its scope, reflecting the novelty of poly(BAAPy) and its limited prior use as a separation material. A dedicated life-cycle assessment (LCA) would enable quantitative evaluation of the overall environmental footprint of the process, including solvent use, energy demand, and polymer preparation/regeneration. In addition, extended regeneration studies over a substantially larger number of adsorption–desorption cycles would be valuable to verify long-term capacity retention, selectivity stability, and regeneration efficiency under repeated operation. Finally, a focused modelling study examining poly(BAAPy) interactions with a broader library of bioactive compounds could deepen mechanistic understanding and support predictive optimisation of polymer design and operating conditions.

Overall, this work offers a sustainable valorisation route for viticultural waste by integrating subfamily-selective polymer adsorption, green solvent use, and simplified downstream processing. The demonstrated performance of poly(BAAPy) advances the development of functional adsorbent materials for scalable, eco-conscious natural product purification, supporting broader goals in circular bioeconomy and environmental chemical engineering.

CRediT authorship contribution statement

Amir Bzainia: Writing – original draft, Investigation, Data curation,

Table 6
Overview of representative studies on the separation of stilbenes from plant-derived matrices. Listed parameters include reported HPLC-based purities and whether stilbene family-/subfamily-level fractionation was achieved, including separation between monomers and oligomers and/or within monomeric and oligomeric subclasses.

Sample type	Target stilbenes	Separation methods	Outcomes	Main Challenges Reported	Stilbene family-level fractionation achieved?*	Reference
Grapevine canes	Monomers: t-piceatannol, t-resveratrol Oligomers: t-ε-viniferin, miyabenol C	Dynamic adsorption-desorption using a synthetic poly(2,6-bis (acrylamido)pyridine) adsorbent	Monomer-rich fractions (85–90 % HPLC purity); oligomer-rich fractions (90 % HPLC purity); achieved through single dynamic cycle	Fine-tuning of the gradient is required to minimize subfamily overlap during stilbene elution	Yes	**This work**
Polygonum multiflorum root	Monomers: 2,3,5,4′-tetrahydroxystilbene-2-O-β-D-glucoside	Dynamic adsorption using macroporous resin (AB-8)	HPLC purity increased from 7.5 % to 64.8 %	Enrichment of TSG complicated by concurrent detoxification	No	[48]
Polygonum multiflorum root	Monomers: 2,3,5,4′-tetrahydroxystilbene-2-O-β-glucopyranoside	Dynamic absorption using macroporous resin (HPD100)	HPLC purity of 81.9 %	Multiple separation steps needed	No	[49]
Pigeon pea Cajanus cajan leaves	Monomers: cajaninstilbene acid (CSA), longistyline C (LLC)	Dynamic absorption using macroporous resins	Enrichment factors of 10.8 × (CSA), 9.0 × (LLC)	Required extensive pre-screening	No	[50]
Vitis chunganenis (wild grape species)	Oligomers: hopeaphenol, amurensin G, vitisin A	HSCCC followed with a stepwise elution	Oligomer-rich fraction with HPLC purity > 95.0 %	Large partition coefficient differences hindered resolution; stepwise elution necessary to overcome system limitations.	Yes	[17]
Seed kernel of Iris lactea Pall. var. chinensis	Monomers: t-ε-viniferin Oligomers: vitisin A, vitisin B, vitisin C (resveratrol tetramers)	Two-step HSCCC	Oligomer-rich fractions with HPLC purity > 95.0 %	Reverse elution mode and solvent system optimization required for full tetramer isolation	Yes	[51]
Grapevine shoots (Vitis vinifera)	Monomers: t-resveratrol, t-piceatannol Oligomers: viniferins, vitisin A/B, ampelopsin A, hopeaphenol, isohopeaphenol, miyabenol C, pallidol	Centrifugal partition chromatography (CPC); preparative HPLC	Oligomer-rich fractions	Complex separation due to structural similarity among stilbenes	Yes	[4]
Vitis vinifera Chardonnay stems	Monomers: t-resveratrol, t-piceatannol Oligomers: viniferins, ampelopsin B, miyabenol C, vitisin A	MtBE fractionation; CPC	HPLC purity of 95.0 %; separate fractions with enrichment of dimers and trimers	Complex solvent system optimization required; dimers and trimers partially resolved only	Partial	[52]
Dipterocarpus semivestitus and Neobalanocarpus heimii heartwood	Oligomers: viniferins, miyabenol C, Ampelopsin C, Hemsleyanol D, Isohopeaphenol	MPLC; semi-preparative HPLC; recycling HPLC	HPLC purities between 92.4 %–98.6 %.	Co-elution and stereoisomer separation difficult; high sample needs; 10–15 chromatographic cycles required	Yes	[15]

* Yes: distinct family-/subfamily-level fractionation was achieved (e.g., monomers vs oligomers and/or separation within monomeric and/or oligomeric subclasses) with clearly differentiated fractions and/or reported purity/enrichment; Partial: some enrichment achieved, but with overlap or unresolved co-elution; No: no clear family-/subfamily-level distinction reported (mainly bulk recovery without differentiated fractions).

Conceptualization. **Dias Rolando:** Writing – review & editing, Validation, Supervision, Project administration, Funding acquisition, Conceptualization. **Erik Keller:** Supervision, Conceptualization. **André Heeres:** Writing – review & editing, Supervision, Conceptualization. **Costa Mário:** Writing – review & editing, Conceptualization.

Declaration of Competing Interest

The authors declare that the research was conducted in the absence of any commercial or financial relationships that could be construed as a potential conflict of interest.

Acknowledgments

We are grateful to the members of the Research Centre Biobased Economy at Hanze University of Applied Sciences for their invaluable support and assistance. We are also thankful for the financial aid provided by "BacchusTech-Integrated Approach for the Valorisation of Winemaking Residues" (POCI-01–0247-FEDER-069583), supported by the Competitiveness and Internationalization Operational Program (COMPETE 2020), under the PORTUGAL 2020 Partnership Agreement, through the European Regional Development Fund (ERDF). Amir Bzainia is grateful to the financial support provided by the Foundation for Science and Technology (FCT, Portugal) through the PhD grant reference of doi.org/10.54499/UI/BD/153688/2022. Rolando C. S. Dias is grateful to the Foundation for Science and Technology (FCT, Portugal) for financial support through national funds FCT/MCTES (PIDDAC) to CIMO (UIDB/00690/2020 and UIDP/ 00690/2020) and SusTEC (LA/P/0007/2020). Mário Rui P. F. N. Costa acknowledges the support by LA/P/0045/2020 (ALiCE), UIDB/50020/2020, and UIDP/50020/2020 (LSRE-LCM), funded by national funds through FCT/MCTES (PIDDAC).

Appendix A. Supporting information

Supplementary data associated with this article can be found in the online version at doi:10.1016/j.jece.2026.121773.

Data availability

Data will be made available on request.

References

[1] C.-G. Duta-Bratu, G.M. Nitulescu, D.P. Mihai, O.T. Olaru, Resveratrol and other natural oligomeric stilbenoid compounds and their therapeutic applications, Plants 12 (16) (Aug. 2023) 2935, https://doi.org/10.3390/plants12162935.

[2] B. DeFilippis, A. Ammazzalorso, M. Fantacuzzi, L. Giampietro, C. Maccallini, R. Amoroso, Anticancer activity of stilbene-based derivatives, ChemMedChem 12 (8) (Apr. 2017) 558–570, https://doi.org/10.1002/cmdc.201700045.

[3] J. Gabaston, et al., Wood and roots of major grapevine cultivars and rootstocks: a comparative analysis of stilbenes by UHPLC-DAD-MS/MS and NMR, Phytochem. Anal. 30 (3) (May 2019) 320–331, https://doi.org/10.1002/pca.2815.

[4] B. Biais, et al., Antioxidant and cytoprotective activities of grapevine stilbenes, J. Agric. Food Chem. 65 (24) (Jun. 2017) 4952–4960, https://doi.org/10.1021/acs.jafc.7b01254.

[5] C. Privat, J.P. Telo, V. Bernardes-Genisson, A. Vieira, J.-P. Souchard, F. Nepveu, Antioxidant properties of *trans* -ε-Viniferin as compared to stilbene derivatives in aqueous and nonaqueous media, J. Agric. Food Chem. 50 (5) (Feb. 2002) 1213–1217, https://doi.org/10.1021/jf010676t.

[6] B. Sy, S. Krisa, T. Richard, A. Courtois, Resveratrol, ε-Viniferin, and Vitisin B from Vine: comparison of their in vitro antioxidant activities and study of their interactions, Molecules 28 (22) (Nov. 2023) 7521, https://doi.org/10.3390/molecules28227521.

[7] Y.-Q. Xue, J.-M. Di, Y. Luo, K.-J. Cheng, X. Wei, Z. Shi, Resveratrol oligomers for the prevention and treatment of cancers, Oxid. Med Cell Longev. 2014 (2014) 1–9, https://doi.org/10.1155/2014/765832.

[8] W.P. Jones and A.D. Kinghorn, "Extraction of Plant Secondary Metabolites," 2012, pp. 341–366. doi: 10.1007/978-1-61779-624-1_13.

[9] J.R. Vergara-Salinas, et al., Effect of Pressurized Hot Water Extraction on Antioxidants from Grape Pomace before and after Enological Fermentation, J. Agric. Food Chem. 61 (28) (Jul. 2013) 6929–6936, https://doi.org/10.1021/jf4010143.

[10] J. Xiao, Recent advances on the stability of dietary polyphenols, eFood 3 (3) (Jun. 2022), https://doi.org/10.1002/efd2.21.

[11] N.S.A. Derkyi, B. Adu-Amankwa, D. Sekyere, N.A. Darkwa, Optimum acetone and ethanol extraction of polyphenols from Pinus caribaea Bark: maximizing tannin content using response surface methodology, Chem. Prod. Process Model. 6 (1) (Feb. 2011), https://doi.org/10.2202/1934-2659.1546.

[12] K. Gaudin, et al., Separation of polyphenols by HILIC methods with diode array detection, charged aerosol detection and mass spectrometry: application to grapevine extracts rich in stilbenoids, J. Chromatogr. A 1736 (Nov. 2024) 465422, https://doi.org/10.1016/j.chroma.2024.465422.

[13] Y. Wei, P. Li, L. Ma, J. Li, Separation and purification of four stilbenes from Vitis vinifera L. cv. cabernet sauvignon roots through high-speed counter-current chromatography, South Afr. J. Enol. Vitic. 35 (2) (Sep. 2016), https://doi.org/10.21548/35-2-1011.

[14] S. He, Y. Lu, L. Jiang, B. Wu, F. Zhang, Y. Pan, Preparative isolation and purification of antioxidative stilbene oligomers from *Vitis chunganeniss* using high-speed counter-current chromatography in stepwise elution mode, J. Sep Sci. 32 (14) (Jul. 2009) 2339–2345, https://doi.org/10.1002/jssc.200900033.

[15] R. Ramli, N.H. Ismail, N. Manshoor, Recycling HPLC for the purification of oligostilbenes from *Dipterocarpus semivestitus* and *Neobalanocarpus heimii* (Dipterocarpaceae), J. Liq. Chromatogr. Relat. Technol. 40 (18) (Nov. 2017) 943–949, https://doi.org/10.1080/10826076.2017.1386673.

[16] E. Sursin, et al., Combining Laccase-mediated dimerization of resveratrol and centrifugal partition chromatography: optimization of E-Labruscol production and identification of new resveratrol dimers, ACS Sustain Chem. Eng. 11 (31) (Aug. 2023) 11559–11569, https://doi.org/10.1021/acssuschemeng.3c01997.

[17] J. Bisson, et al., Development of hybrid elution systems for efficient purification of stilbenoids using centrifugal partition chromatography coupled to mass spectrometry, J. Chromatogr. A 1218 (36) (Sep. 2011) 6079–6084, https://doi.org/10.1016/j.chroma.2011.03.020.

[18] M.S. Akhtar, S. Ali, W. Zaman, Innovative Adsorbents for Pollutant Removal: Exploring the Latest Research and Applications, Molecules 29 (18) (Sep. 2024) 4317, https://doi.org/10.3390/molecules29184317.

[19] K. Zong, K. Jiang, X. Bao, D. Deng, Preparation of highly sulfonated hyper-crosslinked polymers as promising ammonia adsorbents with excellent performance, J. Environ. Chem. Eng. 13 (2) (Apr. 2025) 116082, https://doi.org/10.1016/j.jece.2025.116082.

[20] M. Santhamoorthy, et al., A comprehensive review of the functionalized polymer composite membranes in wastewater treatment, J. Environ. Chem. Eng. 13 (5) (Oct. 2025) 117735, https://doi.org/10.1016/j.jece.2025.117735.

[21] M. Gao, X. Wang, M. Gu, Z. Su, Y. Wang, J. Janson, Separation of polyphenols using porous polyamide resin and assessment of mechanism of retention, J. Sep Sci. 34 (15) (Aug. 2011) 1853–1858, https://doi.org/10.1002/jssc.201100139.

[22] C.P. Gomes, et al., Scale-up of a sorption process working with molecularly imprinted adsorbents for enrichment of winemaking residues and improvement of bioactivity, Clean. Circ. Bioeconomy 8 (Aug. 2024) 100093, https://doi.org/10.1016/j.clcb.2024.100093.

[23] A. Bzainia, G. Igrejas, M.J.V. Pereira, M.R.P.F.N. Costa, R.C.S. Dias, Purification of stilbenes from grape stems in a continuous process based on photo-molecularly imprinted adsorbents and hydroalcoholic solvents, Sep Purif. Technol. 349 (Dec. 2024) 127798, https://doi.org/10.1016/j.seppur.2024.127798.

[24] E. Bilalov, C. Martins, M.R.P.F.N. Costa, R.C.S. Dias, Separation of Bioactive Compounds in Olive Leaf with a Pyridyl-Functionalized Adsorbent and Hydroalcoholic Solvents, Ind. Eng. Chem. Res. 64 (10) (Mar. 2025) 5575–5588, https://doi.org/10.1021/acs.iecr.4c04622.

[25] A. Krzyszczak-Turczyn, M. Grochowicz, I. Jonik, I. Sadok, Removal of polyphenols from anthocyanin-rich extracts using 4-vinylpyridine crosslinked copolymers, Food Chem. 463 (Jan. 2025) 141312, https://doi.org/10.1016/j.foodchem.2024.141312.

[26] C. Gomes, G. Sadoyan, R. Dias, M. Costa, Development of Molecularly Imprinted Polymers to Target Polyphenols Present in Plant Extracts, Processes 5 (4) (Nov. 2017) 72, https://doi.org/10.3390/pr5040072.

[27] C.P. Gomes, R.C.S. Dias, M.R.P.F.N. Costa, Hybrid cellulose-poly(4-vinylpyridine) adsorbents produced via ATRP and their application to target polyphenols in winemaking, olive oil production and almond processing residues, React. Funct. Polym. 164 (Jul. 2021) 104930, https://doi.org/10.1016/j.reactfunctpolym.2021.104930.

[28] A. Bzainia, E. Keller, A. Heeres, M.R.P.F.N. Costa, R.C.S. Dias, Synthesis of a dual-function monomer and its corresponding polymer for the valorisation of stilbenes from grape canes, Eur. Polym. J. 236 (Aug. 2025) 114142, https://doi.org/10.1016/j.eurpolymj.2025.114142.

[29] T. Fundneider, V. Acevedo Alonso, G. Abbt-Braun, A. Wick, D. Albrecht, S. Lackner, Empty bed contact time: The key for micropollutant removal in activated carbon filters, Water Res 191 (Mar. 2021) 116765, https://doi.org/10.1016/j.watres.2020.116765.

[30] A. Betsholtz, P. Falås, O. Svahn, M. Cimbritz, Å. Davidsson, New Perspectives on the Interactions between Adsorption and Degradation of Organic Micropollutants in Granular Activated Carbon Filters, Environ. Sci. Technol. 58 (26) (Jul. 2024) 11771–11780, https://doi.org/10.1021/acs.est.4c00815.

[31] Z.R. Herm, et al., Separation of Hexane Isomers in a Metal-Organic Framework with Triangular Channels, Science (1979) 340 (6135) (May 2013) 960–964, https://doi.org/10.1126/science.1234071.

[32] D. Juela, M. Vera, C. Cruzat, X. Alvarez, E. Vanegas, Mathematical modeling and numerical simulation of sulfamethoxazole adsorption onto sugarcane bagasse in a fixed-bed column, Chemosphere 280 (Oct. 2021) 130687, https://doi.org/10.1016/j.chemosphere.2021.130687.

[33] L. Bavaresco, M. Fregoni, M. Trevisan, F. Mattivi, U. Vrhovsek, R. Falchetti, 2002, Occur. stilbene piceatannol grapes.

[34] Y. Papastamoulis, et al., New E-miyabenol isomer isolated from grapevine cane using centrifugal partition chromatography guided by mass spectrometry, Tetrahedron 71 (20) (May 2015) 3138–3142, https://doi.org/10.1016/j.tet.2014.08.029.

[35] A. Bzainia, R.C.S. Dias, M.R.P.F.N. Costa, Enrichment of Quercetin from Winemaking Residual Diatomaceous Earth via a Tailor-Made Imprinted Adsorbent, Molecules 27 (19) (Sep. 2022) 6406, https://doi.org/10.3390/molecules27196406.

[36] A. Bzainia, R.C.S. Dias, M.R.P.F.N. Costa, A simple process to purify (*E*)-resveratrol from grape stems with a photo-molecularly imprinted sorbent, Food Bioprod. Process 142 (Nov. 2023) 1–16, https://doi.org/10.1016/j.fbp.2023.08.010.

[37] K.Y. Foo, B.H. Hameed, Insights into the modeling of adsorption isotherm systems, Chem. Eng. J. 156 (1) (Jan. 2010) 2–10, https://doi.org/10.1016/j.cej.2009.09.013.

[38] K.H. Chu, M.A. Hashim, Adsorptive removal of pharmaceutical contaminants: Accurate description of tailing breakthrough curves, J. Environ. Chem. Eng. 11 (5) (Oct. 2023) 111025, https://doi.org/10.1016/j.jece.2023.111025.

[39] C. Jiang, X. Gong, H. Qu, Multivariate Modeling and Prediction of Breakthrough Curves for Herbal Medicine Adsorption on Column Chromatography: A Case Study, Sep Sci. Technol. 50 (7) (May 2015) 1030–1037, https://doi.org/10.1080/01496395.2014.978458.

[40] E.R. Azhagiya Singam, et al., Thermodynamics of Adsorption on Graphenic Surfaces from Aqueous Solution, J. Chem. Theory Comput. 15 (2) (Feb. 2019) 1302–1316, https://doi.org/10.1021/acs.jctc.8b00830.

[41] M. Silva, L. Castellanos, M. Ottens, Capture and Purification of Polyphenols Using Functionalized Hydrophobic Resins, Ind. Eng. Chem. Res 57 (15) (Apr. 2018) 5359–5369, https://doi.org/10.1021/acs.iecr.7b05071.

[42] S. Cheng, H. Tang, H. Yan, Effects of multiple weak interactions on the binding of phenolic compounds by polymeric adsorbents, J. Appl. Polym. Sci. 102 (5) (Dec. 2006) 4652–4658, https://doi.org/10.1002/app.24702.

[43] M. Van den Bergh, S. Smolders, D. De Vos, Adsorption, Liquid Separation. Kirk-Othmer Encyclopedia of Chemical Technology, Wiley, 2021, pp. 1–41, https://doi.org/10.1002/0471238961.0104191507051302.a01.pub3.

[44] A.E. Rodrigues, Chemical engineering and environmental challenges. Cyclic adsorption/reaction technologies: Materials and process together!, J. Environ. Chem. Eng. 8 (4) (Aug. 2020) 103926, https://doi.org/10.1016/j.jece.2020.103926.

[45] C. Barjot, M. Tournaire, C. Castagnino, C. Vigor, J. Vercauteren, J.-F. Rossi, Evaluation of antitumor effects of two vine stalk oligomers of resveratrol on a panel of lymphoid and myeloid cell lines: comparison with resveratrol, Life Sci. 81 (23–24) (Nov. 2007) 1565–1574, https://doi.org/10.1016/j.lfs.2007.08.047.

[46] M. Wang, Y. Jin, C.-T. Ho, Evaluation of resveratrol derivatives as potential antioxidants and identification of a reaction product of resveratrol and 2,2-Diphenyl-1-picryhydrazyl Radical, J. Agric. Food Chem. 47 (10) (Oct. 1999) 3974–3977, https://doi.org/10.1021/jf990382w.

[47] J. Gabaston, et al., Stilbenes from *Vitis vinifera* L. waste: a sustainable tool for controlling *Plasmopara Viticola*, J. Agric. Food Chem. 65 (13) (Apr. 2017) 2711–2718, https://doi.org/10.1021/acs.jafc.7b00241.
[48] T. Deng, J. Jia, N. Luo, H. Li, A dual-task method for the simultaneous detoxification and enrichment of stilbene glycoside from Polygonum multiflorum roots extract by macroporous resin, Chem. Eng. J. 237 (Feb. 2014) 138–145, https://doi.org/10.1016/j.cej.2013.10.020.
[49] L. Lv, J. Tang, C. Ho, Selection and optimisation of macroporous resin for separation of stilbene glycoside from *Polygonum multiflorum* Thunb, J. Chem. Technol. Biotechnol. 83 (10) (Oct. 2008) 1422–1427, https://doi.org/10.1002/jctb.1964.
[50] Z. Wei, et al., Resin adsorption as a means to enrich rare stilbenes and coumarin from pigeon pea leaves extracts, Chem. Eng. J. 172 (2–3) (Aug. 2011) 864–871, https://doi.org/10.1016/j.cej.2011.06.075.
[51] H. Lv, H. Wang, Y. He, C. Ding, X. Wang, Y. Suo, Separation and purification of four oligostilbenes from Iris lactea Pall. var. chinensis (Fisch.) Koidz by high-speed counter-current chromatography, J. Chromatogr. B 988 (Apr. 2015) 127–134, https://doi.org/10.1016/j.jchromb.2015.02.035.
[52] N. Zga, et al., Preparative purification of antiamyloidogenic stilbenoids from Vitis vinifera (Chardonnay) stems by centrifugal partition chromatography, J. Chromatogr. B 877 (10) (Apr. 2009) 1000–1004, https://doi.org/10.1016/j.jchromb.2009.02.026.